AD-A066 977 GENERAL ELECTRIC CO SANTA BARBARA CALIF TEMPO F/G 20/14
WEDCOM IV: A FORTRAN CODE FOR THE CALCULATION OF ELF, VLF, AND --ETC(U)
NOV 78 R R RUTHERFORD DNA001-78-C-0043
UNCLASSIFIED GE77TMP-33-VOL-3 DNA-4422T-3 NL

| OF |
AD
A066977

END
DATE
FILMED
8-81
DTIC

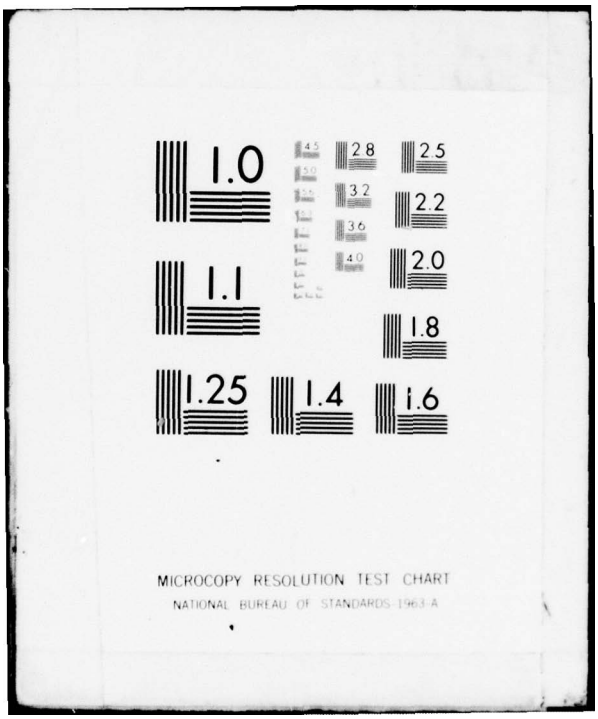
1.0
1.1
1.25
1.4
1.6
1.8
2.0
2.2
2.5
2.8
3.2
3.6
4.0
MICROCOPY RESOLUTION TEST CHART
NATIONAL BUREAU OF STANDARDS 1963-A

DNA 4422T-3

WEDCOM IV: A FORTRAN CODE FOR THE CALCULATION OF ELF, VLF, AND LF PROPAGATION IN A NUCLEAR ENVIRONMENT

Volume III — Computational Models

General Electric Company - TEMPO
Center for Advanced Studies
816 State Street
Santa Barbara, California 93101

1 November 1978

Topical Report for Period 15 October 1977—1 November 1978

CONTRACT No. DNA 001-78-C-0043

THIS WORK SPONSORED BY THE DEFENSE NUCLEAR AGENCY
UNDER RDT&E RMSS CODE B322078464 S99QAXHE04336 H2590D.

Prepared for
Director
DEFENSE NUCLEAR AGENCY
Washington, D. C. 20305

88

Destroy this report when it is no longer needed. Do not return to sender.

PLEASE NOTIFY THE DEFENSE NUCLEAR AGENCY, ATTN: TISI, WASHINGTON, D.C. 20305, IF YOUR ADDRESS IS INCORRECT, IF YOU WISH TO BE DELETED FROM THE DISTRIBUTION LIST, OR IF THE ADDRESSEE IS NO LONGER EMPLOYED BY YOUR ORGANIZATION.

UNCLASSIFIED

SECURITY CLASSIFICATION OF THIS PAGE (When Data Entered)

REPORT DOCUMENTATION PAGE		READ INSTRUCTIONS BEFORE COMPLETING FORM
1. REPORT NUMBER DNA 4422T-3	2. GOVT ACCESSION NO.	3. RECIPIENT'S CATALOG NUMBER
4. TITLE (and Subtitle) WEDCOM IV: A FORTRAN CODE FOR THE CALCULATION OF ELF, VLF, AND LF PROPAGATION IN A NUCLEAR ENVIRONMENT Volume III—Computational Models		5. TYPE OF REPORT & PERIOD COVERED Topical Report for Period 15 Oct 77—1 Nov 78 6. PERFORMING ORG. REPORT NUMBER GE77TMP-33
7. AUTHOR(s) Royden R. Rutherford		8. CONTRACT OR GRANT NUMBER(s) DNA 001-78-C-0043
9. PERFORMING ORGANIZATION NAME AND ADDRESS General Electric Company—TEMPO, Center for Advanced Studies, 816 State Street Santa Barbara, California 93101		10. PROGRAM ELEMENT, PROJECT, TASK AREA & WORK UNIT NUMBERS NWED Subtask S99QAXHE043-36
11. CONTROLLING OFFICE NAME AND ADDRESS Director Defense Nuclear Agency Washington, D.C. 20305		12. REPORT DATE 1 November 1978 13. NUMBER OF PAGES 94
14. MONITORING AGENCY NAME & ADDRESS(if different from Controlling Office)		15. SECURITY CLASS. (of this report) UNCLASSIFIED 15a. DECLASSIFICATION DOWNGRADING SCHEDULE

16. DISTRIBUTION STATEMENT (of this Report)

Approved for public release; distribution unlimited.

17. DISTRIBUTION STATEMENT (of the abstract entered in Block 20, if different from Report)

18. SUPPLEMENTARY NOTES

This work sponsored by the Defense Nuclear Agency under RDT&E RMSS Code B322078464 S99QAXHE04336 H2590D.

19. KEY WORDS (Continue on reverse side if necessary and identify by block number)

Nuclear Weapon Effects
ELF Propagation
VLF Propagation
LF Propagation

20. ABSTRACT (Continue on reverse side if necessary and identify by block number)

This document describes electromagnetic propagation computational models used in WEDCOM IV, a computer code that calculates ELF, VLF, and LF electric and magnetic field strengths in nuclear-disturbed environments. The code replaces the previous version of the WEDCOM code (WEDCOM III) documented in DNA 2875F.

DD FORM 1 JAN 73 1473 EDITION OF 1 NOV 65 IS OBSOLETE

UNCLASSIFIED

SECURITY CLASSIFICATION OF THIS PAGE (When Data Entered)

CONTENTS

ILLUSTRATIONS

TABLES

SECTION 1
INTRODUCTION

The WEDCOM code is a digital computer program that calculates ELF, VLF, and LF electric and magnetic field strengths in ambient and nuclear-disturbed environments. The code is intended for use when a relatively detailed analysis of the propagation between two terminals is required in nuclear-disturbed environments. The code can be used alone to study the effects of weapon, atmosphere, and propagation parameters on received signals or can be used in conjunction with receiver antenna and signal processing models to evaluate system performance.

Operational information for WEDCOM IV is given in Volume 1 (User's Manual). A description of computer routines used to model ELF, VLF, and LF propagation is given in Volume 2 (Computer Routines). This volume (Volume 3) provides mathematical descriptions of the propagation models in a manner that does not presume knowledge of the internal organization of the WEDCOM code or Fortran programming in general.

The ambient and nuclear environment models used in WEDCOM are taken directly from the WEPH VI code. These models are described in Reference 1-1 and are not further discussed here. The propagation computational models used in WEDCOM IV include models developed for WEDCOM III, models developed for DCOM (a code developed for the MEECN office), and models developed by the Naval Ocean Systems Center (NOSC). Descriptions of models developed for the DCOM code have been taken from the DCOM code documentation (Reference 1-2). Description of models developed by NOSC have been obtained from References 1-3 and 1-4.

A description of reflection coefficient models used for ELF, VLF, and LF propagation is given in Section 2. Section 3 describes the waveguide model used for ELF and VLF propagation and Section 4 describes the skywave model used for LF propagation. Introductory information concerning propagation model limitations, coordinate systems, and matrix notation is given below.

MODEL LIMITATIONS

It should be noted that there are potentially significant physical processes that either are not treated or are very crudely modeled, since they either have been regarded as being of secondary importance in past applications or have not yet been modeled adequately.

The calculation of ELF propagation characteristics is difficult due to the long wavelengths involved. In particular, ionospheric variations transverse to the propagation path are not modeled and, as a result, predicted degradation is probably pessimistic. Standard WKB approximations, which assume a slow variation in ionospheric or ground electrical properties in the direction of propagation, are used. In addition, there is some uncertainty in selecting the appropriate combinations of D-, E-, and lower F-region ionospheric models for ELF predictions.

Propagation variations transverse to the propagation paths are also ignored for VLF, but this limitation is not as severe as for ELF because of the relatively short VLF wavelengths.

The LF model is an approximate ray theory model using correction factors for diffraction around the earth's bulge. The effects of the geomagnetic field are included in the reflection coefficient calculation, and a geometric search procedure accommodates nonuniformities in the ionosphere in the direction of propagation. The model has produced good agreement with calculations performed with state-of-the-art models and assuming a uniform ionosphere for frequencies between 20 and 60 kHz.

COORDINATE SYSTEM AND ANTENNA REFERENCE

Many calculations performed by the system models are performed with geometry references to a specified location, in this report referred to as a Computation Reference Point (CRP). The Cartesian coordinate system is the most frequently used geometry system. In this report,

x = direction of propagation path (km)
y = perpendicular to direction of propagation path (km)
z = altitude (km).

The origin is at the earth's surface.

The propagation models assume that the radiated power is defined. For VLF and LF, total power radiated from a dipole with a particular orientation may be specified. The antenna zenith angle (γ) and orientation relative to the propagation path (ϕ) are shown in Figure 1-1. For ELF, the total power and ϕ are specified, and γ is always 90 degrees.

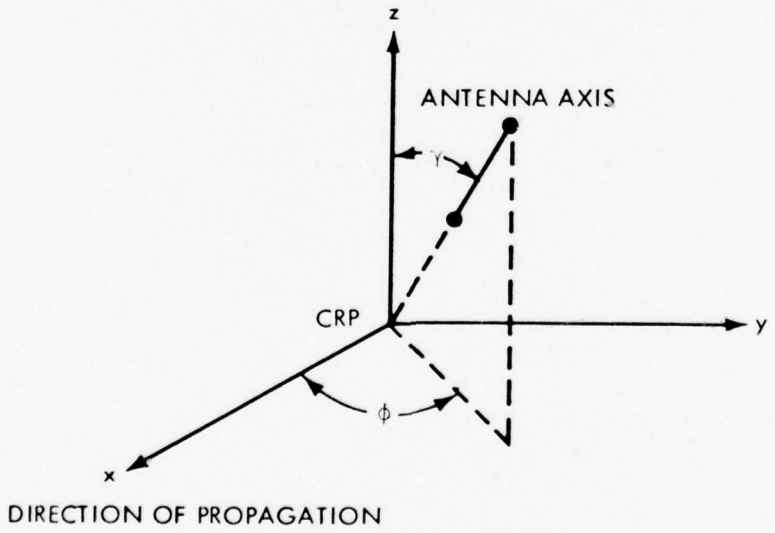

Figure 1-1. Coordinate system and antenna orientation.

MATRIX NOTATION

A square matrix will be denoted by an underlined symbol. Matrix elements will be subscripted as demonstrated here by the $\underline{M}$ matrix:

$$\underline{M} = \begin{bmatrix} M_{11} & M_{12} & M_{13} \\ M_{21} & M_{22} & M_{23} \\ M_{31} & M_{32} & M_{33} \end{bmatrix} . \qquad (1\text{-}1)$$

REFERENCES

1-1 Knapp, W.S., *WEPH VI: A Fortran Code for the Calculation of Ionization and Electromagnetic Propagation Effects due to Nuclear Detonations, Volume 2, Computer Routines*, GE75TMP-53, General Electric—TEMPO, October 1976.

1-2 Feniger, E.J., *MEECN Nuclear Effects Systems Codes, Volume 2, DCOM Code: User's Guide*, GE75TMP-9, General Electric—TEMPO, June 1975.

1-3 Morfitt, D.G., and C.H. Shellman, *MODESRCH, An Improved Computer Program for Obtaining ELF/VLF/LF Mode Constants in an Earth-Ionosphere Waveguide*, Interim Report No. 77T, Naval Electronics Laboratory Center, San Diego, California, October 1976.

1-4 Pappert, R.A., and L.R. Shockey, *WKB Mode Summary Program for VLF/ELF Antennas of Arbitrary Length, Shape, and Elevation*, Interim Report 715, Naval Electronics Laboratory Center, San Diego, California, June 1971.

SECTION 2
IONOSPHERIC REFLECTION COEFFICIENTS

INTRODUCTION

Both waveguide and ray theory solutions require that ionospheric reflection coefficients (ratio of the reflected field to the incident field) be computed. The ionospheric reflection coefficients can be represented as a four-component matrix, ie,

$$\underline{R} = \begin{bmatrix} {}_{\parallel}R_{\parallel} & {}_{\perp}R_{\parallel} \\ {}_{\parallel}R_{\perp} & {}_{\perp}R_{\perp} \end{bmatrix} , \tag{2-1}$$

where

$\underline{R}$ is the reflection coefficient matrix

$\parallel$ means polarization parallel to the plane of incidence

$\perp$ means polarization perpendicular to the plane of incidence.

The first subscript applies to the polarization of the incident wave, and the second subscript applies to the polarization of the reflected wave.

The coupling coefficients, ${}_{\perp}R_{\parallel}$ and ${}_{\parallel}R_{\perp}$, may be as large or larger than the primary coefficients ${}_{\parallel}R_{\parallel}$ and ${}_{\perp}R_{\perp}$ for normal nighttime, but they are typically much smaller than the primary coefficients for daytime conditions. For a normal ionosphere, the coefficients are a function of propagation azimuth and the earth's magnetic field. A nuclear disturbance results in lowering the reflection region; as a consequence of the increased electron-neutral collision frequency in the reflecting region, a strong disturbance can cause the coupling coefficients to be essentially zero.

LF and VLF waves are reflected from the D-region. Most of the reflected energy is returned from the 60-70 km altitude level for normal daytime ionospheres and from 80-90 km altitude level for normal nighttime ionospheres. In these altitude ranges, particularly for nighttime conditions, the electron-neutral collision frequency is comparable to the electron gyrofrequency, and the earth's magnetic field has a significant effect on the reflection coefficient.

ELF reflection coefficients are affected by ionization in the E- and F-regions in addition to ionization in the D-region. Thus, effects from the earth's magnetic field are always important. The ion concentrations from ground level up to the D-region also affect the ELF reflection coefficient values.

The WEDCOM code employs two calculation procedures for determining the ionospheric reflection coefficients. The first method is an iterative integration of a first-order differential equation (Reference 2-1). It is applicable to both isotropic and anisotropic ionospheres. The second procedure is an application of a simple recursive technique (Reference 2-2) and is used only with isotropic ionospheres.

Both reflection coefficient computation procedures allow for arbitrary vertical profiles for electron and ion densities. These profiles are divided into horizontal slabs. The iterative integration method allows a simple variation of the the slab electromagnetic properties. This procedure is used for all ELF cases and for VLF and LF cases where the ionosphere is highly disturbed. The recursive technique requires less computation time than the iterative integration method.

COMPUTATION OF REFLECTION COEFFICIENTS FOR ANISOTROPIC IONOSPHERE

The reflection coefficient calculation technique described by Budden (Reference 2-1) is used here. The model is patterned after that described by Sheddy et al (References 2-3 and 2-4).

All ionospheric and geomagnetic-dependent inputs are calculated prior to execution of the model. A fictitious linear variation of the permittivity with altitude is used to simulate the earth curvature.

Basic Equations Defining $\underline{R}$

The ionospheric reflection coefficient matrix defined in Equation 2-1 is found by the numerical integration of differential equations of the matrix form

$$2j\underline{R}' = \underline{S}_{21} + \underline{S}_{22}\underline{R} - \underline{R}\,\underline{S}_{11} - \underline{R}\,\underline{S}_{12}\underline{R} \quad , \tag{2-2}$$

where the prime represents the derivative with respect to the normalized parameter kz, and

k = wavenumber (km^{-1})

z = altitude (km) .

The elements of matrix $\underline{S}$ are partitioned for convenience, with the partitioned values being

$$\underline{S}_{11} = \begin{bmatrix} (S_{11a} + S_{11b}) & -S_{12} \\ -S_{21} & S_{22} \end{bmatrix} \tag{2-3a}$$

$$\underline{S}_{12} = \begin{bmatrix} (-d_{11a} + d_{11b}) & -S_{12} \\ -d_{21} & -d_{22} \end{bmatrix} \tag{2-3b}$$

$$\underline{S}_{21} = \begin{bmatrix} (-d_{11a} - d_{11b}) & d_{12} \\ S_{21} & d_{22} \end{bmatrix} \tag{2-3c}$$

$$\underline{S}_{22} = \begin{bmatrix} (S_{11a} - S_{11b}) & d_{12} \\ d_{21} & -S_{22} \end{bmatrix} \quad . \tag{2-3d}$$

The elements of the partitioned S matrix are functions of the ionospheric properties, the geomagnetic field strength, the wave frequency, and the angle of incidence of the wave with the ionosphere.

These matrix elements are defined in Appendix A in terms of an intermediate matrix $\underline{T}$ and the susceptibility matrix $\underline{M}$.

Considerable simplification occurs in the $\underline{S}$, I, and $\underline{M}$ matrices when the geomagnetic field has a negligible influence on the susceptibility matrix. In the WEDCOM code it is assumed that the altitude range where the magnetic field influence is negligible where

$$\left(\frac{Y}{Z}\right)^2 < 10^{-2} \tag{2-4}$$

where

$$Y = \frac{\mu_0 eH}{\omega m}$$

$$Z = 1 - j\,\frac{\nu_e}{\omega}$$

μ_0 = free-space permeability (henry/m)

e = electron charge (coulomb)

H = static magnetic field strength (oersted)

m = electron mass (kg)

ω = frequency (radians s^{-1})

ν_e = electron-neutral collision frequency (s^{-1})

$j = \sqrt{-1}$.

The lower altitude is determined entirely by electrons. The contribution of Y of the normal positive and negative ion concentrations is much smaller than the electron component.

VLF AND LF CASES. Expanding Equation 2-2, equations are written for the four components of the reflection coefficients as they are computed for VLF and LF cases:

$$\begin{aligned} 2j\,{}_{\parallel}R'_{\parallel} = {} & \left[-2S_{11b} + S_{12}\,{}_{\parallel}R_{\perp} + {}_{\perp}R_{\parallel}\,d_{21} + {}_{\parallel}R_{\parallel}(d_{11a} - d_{11b})\right]{}_{\parallel}R_{\parallel} \\ & + \left[{}_{\perp}R_{\parallel}\,{}_{\parallel}R_{\perp}\,d_{22} + {}_{\perp}R_{\parallel}S_{21} + d_{12}\,{}_{\parallel}R_{\perp}\right. \\ & \left. - (d_{11a} + d_{11b})\right] \end{aligned} \tag{2-5a}$$

$$2j\,{}_{\perp}R'_{\parallel} = \left[S_{11a} - S_{11b} + {}_{\parallel}R_{\parallel}(d_{11a} - d_{11b}) - S_{22} + {}_{\perp}R_{\parallel}\,d_{21} + d_{22}\,{}_{\perp}R_{\perp}\right]{}_{\perp}R_{\parallel} + \left[d_{12}(1 + {}_{\perp}R_{\perp}) + {}_{\parallel}R_{\parallel}\,S_{12}(1 + {}_{\perp}R_{\perp})\right] \quad (2\text{-}5b)$$

$$2j\,{}_{\parallel}R'_{\perp} = \left[{}_{\parallel}R_{\parallel}(d_{11a} - d_{11b}) + S_{12}\,{}_{\perp}R_{\parallel} + {}_{\perp}R_{\perp}\,d_{22} - (S_{11a} + S_{11b}) - S_{22}\right]{}_{\parallel}R_{\perp} + \left[S_{21}(1 + {}_{\perp}R_{\perp} + {}_{\parallel}R_{\parallel}\,d_{21}(1 + {}_{\perp}R_{\perp})\right] \quad (2\text{-}5c)$$

$$2j\,{}_{\perp}R'_{\perp} = \left[d_{22}\,{}_{\perp}R_{\perp} - 2S_{22} + {}_{\perp}R_{\parallel}\,d_{21} + S_{12}\,{}_{\parallel}R_{\perp}\right]{}_{\perp}R_{\perp} + \left[d_{22} + {}_{\perp}R_{\parallel}\,{}_{\parallel}R_{\perp}(d_{11a} - d_{11b}) + {}_{\parallel}R_{\perp}\,S_{12} + {}_{\perp}R_{\parallel}\,d_{21}\right] \quad (2\text{-}5d)$$

where $j = \sqrt{-1}$.

ELF CASES. Numerical difficulties can occur when using Equation 2-5 for ELF reflection coefficient calculation. The numerical difficulties result from short computer word length. Using double precision techniques or computers possessing larger word lengths eliminates the problem. A separate algorithm was formulated for WEDCOM for computational efficiency and adaptability to machine type. The scaling and factorization of the reflection coefficient equations are based on the following observations:

1. The $\underline{S}$ matrix elements are large (of order 10^6) at ELF. Also,

$$S_{11b} \approx -d_{11b} \approx CT_{41}$$

$$S_{12} \approx -d_{12} \approx T_{42}$$

$$S_{21} \approx -d_{21} \approx T_{31}$$

$$S_{22} \approx d_{22} \approx T_{21}/C$$

where C is the cosine of the angle of incidence.

2. The diagonal elements of the $\underline{R}$ matrix are characteristically

$$ {}_{\parallel}R_{\parallel} \approx -{}_{\perp}R_{\perp} \approx 1 \quad , \tag{2-6}$$

and the coupling elements ${}_{\perp}R_{\parallel}$ and ${}_{\parallel}R_{\perp}$ are much smaller than unity.

These observations show that subtraction of large, nearly equal values occurs frequently in Equation 2-5. They also provide the basis for modification of Equation 2-5 for computational efficiency.

For ELF cases, Equation 2-5 is modified so that the derivative of the logarithm of R is integrated, where

$$(\ell n\ R)' = \frac{R'}{R} \quad . \tag{2-7}$$

Equation 2-5 is further modified employing the observation noted in Equation 2-6. First, the following relationships are made:

$$ {}_{\parallel}R_{\parallel} = 1 - \Delta_1 \tag{2-8}$$

and

$$ {}_{\perp}R_{\perp} = \Delta_2 - 1 \quad . \tag{2-9}$$

Substitution of Equations 2-8 and 2-9 is made into Equation 2-5. After simplification of terms,

$$\begin{aligned} 2j\,\frac{{}_{\parallel}R'_{\parallel}}{{}_{\parallel}R_{\parallel}} = {} & -4T_{14}/C + 2/{}_{\parallel}R_{\parallel}\left[{}_{\parallel}R_{\perp}T_{12}/C + {}_{\perp}R_{\parallel}T_{34}/C\right] - \Delta_1/{}_{\parallel}R_{\parallel} \\ & \times\left[{}_{\perp}R_{\parallel}\,d_{21} + {}_{\perp}R_{\parallel}S_{21} + 2d_{11a} - \Delta_1(d_{11a} - d_{11b})\right] \\ & + \frac{{}_{\perp}R_{\parallel}\,{}_{\parallel}R_{\perp}}{{}_{\parallel}R_{\parallel}}\,d_{22} \end{aligned} \tag{2-10a}$$

$$2j \frac{{}_{\perp}R'_{\perp}}{{}_{\perp}R_{\perp}} = -4C + \frac{{}_{\perp}R_{\parallel}\,{}_{\parallel}R_{\perp}}{{}_{\perp}R_{\perp}} (d_{11a} - d_{11b}) + \frac{\Delta_2}{{}_{\perp}R_{\perp}} ({}_{\perp}R_{\parallel}\, d_{21} + {}_{\parallel}R_{\perp}\, S_{12} + \Delta_2 d_{22}) \qquad (2\text{-}10b)$$

$$2j \frac{{}_{\perp}R'_{\parallel}}{{}_{\perp}R_{\parallel}} = 2(T_{11} - T_{14}/C - C) - \Delta_1(d_{11a} - d_{11b}) + \Delta_2 d_{22} + {}_{\perp}R_{\parallel} d_{21} + \frac{\Delta_2}{{}_{\perp}R_{\parallel}} (2T_{12}/C - \Delta_1 S_{12}) \qquad (2\text{-}10c)$$

$$2j \frac{{}_{\parallel}R'_{\perp}}{{}_{\parallel}R_{\perp}} = -2(T_{44} + T_{14}/C + C) - \Delta_1(d_{11a} - d_{11b}) + {}_{\parallel}R_{\perp} S_{12} + \Delta_2 d_{22} + \frac{\Delta_2}{{}_{\parallel}R_{\perp}} (2T_{34}/C - \Delta_1 D_{21} \quad . \qquad (2\text{-}10d)$$

The "T" elements in Equations 2-10 belong to an intermediate matrix which relates the susceptibility matrix, $\underline{M}$, to the $\underline{S}$ matrix. The $\underline{T}$ and $\underline{M}$ matrices are defined in Appendix A. Implementation of Equation 2-10 for ELF cases removes the numerical difficulties described earlier.

Integration Technique

The integration technique is that defined in Reference 2-3. It is performed using a fourth-order Runge-Kutta technique. The integrand after n+1 steps is defined by

$$4\underline{R}_{n+1} = \underline{R}_n + \frac{1}{6} (\delta\underline{R}_1 + 2\delta\underline{R}_2 + 2\delta\underline{R}_3 + \delta\underline{R}_4) \quad , \qquad (2\text{-}11)$$

where

$$\delta\underline{R}_1 = -\Delta_z \underline{R}' (z_n, \underline{R}_n)$$

$$\delta\underline{R}_2 = -\Delta_z \underline{R}' (z_n - \frac{\Delta_z}{2} , \underline{R}_n + \delta\underline{R}_1/2)$$

$$\delta \underline{R}_3 = -\Delta_z \underline{R}' \left(z_n - \frac{\Delta_z}{2} , \underline{R}_n + \delta \underline{R}_2/2\right)$$

$$\underline{R}_4 = \Delta_z \underline{R}' \left(z_n - \frac{\Delta_z}{2} , \underline{R}_n + \delta \underline{R}_3\right)$$

Δ_z = step size (km)

$\underline{R}_n$ = integrand after n steps,

and the derivatives are computed using Equation 2-5 or 2-10.

In addition, the integrand is computed using a second-order Runge-Kutta technique, where

$$2\underline{R}_{n+1} = \underline{R}_n - \Delta_z \underline{R}' \left[z_n - \frac{\Delta_z}{2} , \underline{R}_n - \frac{\Delta_z}{2} \underline{R}'(z_n \underline{R}_n)\right] \quad . \qquad (2\text{-}12)$$

Note that the quantities required to calculate the second-order values are already available from the fourth-order calculation. The difference between $4\underline{R}_{n+1}$ and $2\underline{R}_{n+1}$ is used to control the integration step size; that is,

- If $|^2\underline{R}_{n+1} - {}^4\underline{R}_{n+1}| < E_{min}$, the step size is doubled
- If $E_{min} < |^2\underline{R}_{min} - {}^4\underline{R}_{n+1}| < E_{max}$, the step size is unchanged
- If $E_{max} < |^2\underline{R}_{n+1} - {}^4\underline{R}_{n+1}|$, the step size is halved,

and E_{min} and E_{max} are assugned values determined by trial and error calculations. The specified values were selected to assure acceptable accuracy consistent with minimum computing time. Suitable values for E_{max} and E_{min} were found to be:

$$E_{max} = 10^{-2} \qquad (2\text{-}13)$$

$$E_{min} = 10^{-3} \quad . \qquad (2\text{-}14)$$

Integration of Equation 2-5 or 2-10 is carried out by starting at a high enough altitude (defined as z_{top}) and integrating downward, each step employing the control criteria defined above. Integration is terminated based on a criterion which indicates that a free-space assumption can apply (defined as z_{bot}).

During the integration, the step size is controlled by the procedure described above: However, the step size is never allowed to be less than Δz_{min}. A suitable value of Δz_{min} was found to be:

$$\Delta z_{min} = 2 \times 10^{-3} \lambda_0 \quad , \tag{2-15}$$

where λ_0 is the free-space wavelength.

Initial Values for $\underline{R}$

The altitude z_{top} representing the ionosphere top is taken high enough so that reflection from higher altitudes is negligible. The ionosphere is approximated as a uniform semi-infinite anisotropic slab above the top altitude, and thus only upgoing waves exist. The initial step is to determine $\underline{R}$ at z_{top}. The procedure used here is that of Sheddy (Reference 2-5), and the details are included in Appendix B.

Initial Values of z_{top} and z_{bot}

The integration starting altitude z_{top} has a strong influence on the computational efficiency. Factors of 2 to 10 in computational efficiency can be gained, without sacrificing accuracy, by the selection of the proper starting altitude.

The electromagnetic wave behavior in free-space can be treated analytically. Thus, additional computational efficiency is gained by defining the integration stopping altitude, z_{bot}, as the highest altitude where the free-space assumption can be made.

VLF AND LF CASES. The WEDCOM D-region ionization profile is defined up to 100 km. A satisfactory starting altitude criterion applicable for all undisturbed profiles could not be determined. However,

the reflection coefficient values are often affected by the 90-100 km regions. Thus for all VLF undisturbed ionosphere cases, z_{top} is given a value of 100 km. For all other cases, the value of z_{top} is determined by the following procedure.

A satisfactory test for the upper altitude, z_{top}, is based on the value of the imaginary part of the squared index of refraction. The (isotropic) square index of refraction is written as

$$\eta^2(z) = 1 - A - jB \quad , \tag{2-16a}$$

where

$$A = A_e + A_i \tag{2-16b}$$

$$B = B_e + B_i \tag{2-16c}$$

$$A_e = \frac{3.18 \times 10^9 N_e}{\omega^2 + \nu_e^2}$$

$$A_i = \frac{5.45 \times 10^4 N_i}{\omega^2 + \nu_i^2}$$

$$B_e = \frac{\nu_e}{\omega} A_e$$

$$B_i = \frac{\nu_i}{\omega} A_i$$

ν_e = electron-neutral collision frequency (s^{-1})

ν_i = ion-neutral collision frequency (s^{-1})

N_e = electron density (cm^{-3})

N_i = ion density (cm^{-3})

ω = frequency (radians s^{-1}) .

The ionosphere top for VLF/LF cases is defined as that altitude above which

$$B > 2 \text{ maximum } \left[1.0,\ 10\ \frac{\omega}{\nu_e}\right] \quad . \tag{2-17}$$

The ionosphere bottom is defined as that altitude below which

$$B < 0.00022 \quad . \tag{2-18}$$

ELF CASES. Ions at altitudes are important at ELF, and the ionosphere bottom altitude, z_{bot}, is set to ground level. Determination of the upper (starting) altitude, z_{top}, is more complex. Defining z_{top} too high increases the computation time considerably without adding accuracy. Moreover, the algorithm used in VLF/LF cases for determining z_{top} has little value here, as it is more applicable for D-region effects and not for the E- and F-regions where magnetic field effects are strong. The algorithm used in WEDCOM uses an anisotropic definition of the squared index of refraction, Equations 2-16, where for the ordinary wave (see Reference 2-6)

$$A_e = \frac{\omega N_e (\omega + \omega_{me})}{\omega \left[(\omega + \omega_{me})^2 + \nu_e^2\right]}$$

$$A_i = \frac{\omega N_i^2 (\omega + \omega_{ma})}{\omega \left[(\omega + \omega_{ma})^2 + \nu_i^2\right]}$$

$$B_e = \frac{\omega N_e \nu_e}{\omega \left[(\omega + \omega_{me})^2 + \nu_e^2\right]}$$

$$B_i = \frac{\omega N_i^2 \nu_i}{\omega \left[(\omega + \omega_{ma})^2 + \nu_i^2\right]}$$

and

$$\omega_{N_e}^2 = 3.18 \times 10^9 \, N_e \quad \text{(radians s}^{-1}\text{)}$$

$$\omega_{me} = 1.76 \times 10^{11} \, B_m \quad \text{(radians s}^{-1}\text{)}$$

$$\omega_{N_i}^2 = 5.42 \times 10^4 \, N_i \quad \text{(radians s}^{-1}\text{)}$$

$$\omega_{ma} = 3.3 \times 10^6 \, B_m \quad \text{(radians s}^{-1}\text{)}$$

B_m = earth's magnetic field (gauss) .

The WEDCOM ELF model defines z_{top} as the altitude where the transmission loss due to nondeviate incremental absorption satisfies

$$\int_0^{z_{top}} \alpha_T \, dz = 30.0 \qquad (2\text{-}19)$$

and

$$\alpha_T = 8.686 \, \frac{\omega}{c} \, Im(\eta)$$

c = velocity of light (km/s)

$Im(\eta)$ = imaginary part of the index of refraction.

If Equation 2-19 is not satisfied up to 200 km, then z_{top} is given the value of 200 km.

REFLECTION COEFFICIENTS FOR ISOTROPIC IONOSPHERE

General

The reflection coefficients for an isotropic ionosphere are calculated using a method described by Wait (Reference 2-2). Earth curvature and magnetic field effects are ignored. The cross terms of $\underline{R}$ ($_{\perp}R_{\parallel}$ and $_{\parallel}R_{\perp}$) are zero, and the diagonal elements ($_{\parallel}R_{\parallel}$ and $_{\perp}R_{\perp}$) are calculated independently of one another. The following relationships are defined for convenience to help avoid duplication of similar equations:

$$r_v \equiv {}_{\parallel}R_{\parallel}$$

$$r_h \equiv {}_{\perp}R_{\perp} \quad . \tag{2-20}$$

The ionized layer is represented by homogeneous slabs as shown in Figure 2-1, where the wave is incident on the layer bottom by angle ϕ_i and

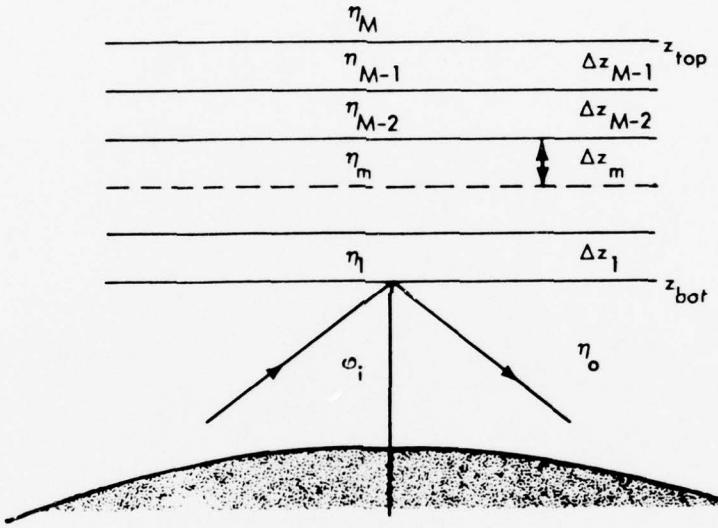

Figure 2-1. Plane wave incident on stratified medium with homogeneous slabs.

η_m = refractive index of mth slab
η_o = refractive index of free space = unity
Δz_m = thickness of mth slab
z_{top} = altitude above which there are no downcoming waves
z_{bot} = altitude at which profile is truncated.

The region below the stratified medium is considered to be free space.

By imposing the condition that the Mth slab is semifinite, only upgoing waves are allowable in the Mth slab and a recursive solution for the reflection coefficient is obtained.

For either a vertically or horizontally polarized plane wave incident on the bottom of a stratified medium, the reflection coefficient (ratio of downgoing to upgoing wave amplitude) is defined as

$$r_{v,h} = \frac{K_o - Z_1}{K_o + Z_1} \quad , \tag{2-21}$$

where K_o is the zeroth term in a series of K_m's and Z_1 is the first term in a series of Z_m's.

K_m is a function of the squared index of refraction of the mth slab:

$$K_m = \begin{cases} \dfrac{b_m}{j\omega\xi_o\eta_m^2} & \text{for vertical polarization} \\ \dfrac{jb_m}{\omega\mu_o} & \text{for horizontal polarization} \end{cases} \tag{2-22}$$

where

$$b_m = \frac{\omega}{c}\sqrt{\sin^2\phi_i - \eta_m^2} \quad . \tag{2-23}$$

K_o, a characteristic impedance of free space, is simply defined as

$$K_o = \begin{cases} \dfrac{\cos\phi_i}{\xi_o c} & \text{for vertical polarization} \\ \dfrac{\cos\phi_i}{\mu_o c} & \text{for horizontal polarization} \quad . \end{cases} \tag{2-24}$$

The series of Z_m's is defined as

$$Z_1 = K_1 \frac{Z_2 + K_1 \tanh b_1 \Delta z_1}{K_1 + Z_2 \tanh b_1 \Delta z_1} \quad (2\text{-}25a)$$

$$Z_m = K_m \frac{Z_{m+1} + K_m \tanh b_m \Delta z_m}{K_m + Z_{m+1} \tanh b_m \Delta z_m} \quad (2\text{-}25b)$$

$$Z_{m-1} = K_{m-1} \frac{Z_m + K_{m-1} \tanh b_{m-1} \Delta z_{m-1}}{K_{m-1} + Z_m \tanh b_{m-1} \Delta z_{m-1}} \quad (2\text{-}25c)$$

$$Z_m = K_m \quad . \quad (2\text{-}25d)$$

In the above equations,

ξ_o = permittivity of free space (farads m^{-1})
c = velocity of light (m s^{-1}) .

The solution is obtained by starting at the Mth slab, computing K_M and K_{M-1}, from them computing Z_{M-1} (using Equation 2-25d to define Z_M), and then proceeding downward, repeating the procedure (using Equations 2-25a, 2-25b, and 2-25c) until a suitable point for truncating the stratified medium is reached.

Analytic Representation of Isotropic Reflection Coefficient

Depressed ionospheres produce reflection coefficients with little magnetic field dependence. Moreover, earth curvature effects are reduced. An analytic representation of the isotropic reflection coefficient is applicable for these cases, and its use can result in considerable saving in computation time.

This approximate formulation is a modified form of that suggested by Wait (References 2-7 and 2-8). It is especially convenient for use in the VLF mode solutions, which require an analytical expression for the reflection coefficient.

The reflection coefficients are calculated for fixed angles of incidence and are represented by

$$r_i(C') = -\exp(\alpha_1 C') \exp\left\{ j\left[\alpha_2 C' + \alpha_3 (C')^2\right]\right\} \quad , \qquad (2\text{-}26)$$

where C' is the cosine of the angle of incidence at the ionosphere and the 's are determined as follows. Reflection coefficients are calculated for two real angles of incidence with cosines C'_1 and C'_2 . If

$$r_i(C'_1) = |r_1| \exp(j\Phi_1) \quad , \qquad (2\text{-}27)$$

$$r_i(C'_2) = |r_2| \exp(j\Phi_2) \quad , \qquad (2\text{-}28)$$

where Φ_1 and Φ_2 are the phases (radians) referred to the same reference altitude, z_R, then

$$\alpha_1 = 1/2\left[\frac{\ln|r_1|}{C'_1} + \frac{\ln|r_2|}{C'_2}\right] \qquad (2\text{-}29)$$

$$\alpha_2 = \alpha_{21} - \alpha_3 C'_1 \qquad (2\text{-}30)$$

$$\alpha_3 = \frac{\alpha_{21} - \alpha_{22}}{C'_1 - C'_2} \quad , \qquad (2\text{-}31)$$

where

$$\alpha_{21} = \frac{\Phi_1 + \pi}{C'_1} \qquad (2\text{-}32)$$

$$\alpha_{22} = \frac{\Phi_2 + \pi}{C'_2} \quad . \qquad (2\text{-}33)$$

The phase of the isotropic reflection coefficient is referenced to the bottom of the ionosphere. To use the analytical reflection coefficient representation just described, the phase must be referenced to the same altitude for all incident angles of interest. The phase reference altitude is determined from the altitude-dependent refractive index.

When the altitude variation of $\eta^2(z)$ is dominated by variations in B(z) (see Equation 2-16), reflection maximizes (Reference 2-9) at approximately the altitude z_R, where

$$B(z_R) = 2 \cos^2 \phi_i \quad , \tag{2-34}$$

where ϕ_i is the angle of incidence at the ionosphere.

A fixed reference altitude is required, and a suitable value is defined by

$$B(z_R) = 0.04 \tag{2-35}$$

by noting that cos ϕ_i for angles of interest is near the range 0.1 to 0.2 .

The exact altitude used for the phase reference altitude is not critical. The calculation procedures are defined so that variations in z_R that are not large relative to z_R have little effect on the final answer. The phase of the reflection coefficient, referred to the reference altitude, is

$$\phi_R = \phi_{min} + 2k \cos \phi_i (z_R - z_{bot}) \quad , \tag{2-36}$$

where

ϕ_R = phase referred to reference altitude (radians)

z_{bot} = altitude where the recursive solution is stopped (km)

ϕ_{min} = phase at z_{bot} returned from recursive calculations (radians).

REFERENCES

2-1 Budden, J.G., "The Numerical Solution of Differential Equations Governing Reflection of Long Radio Waves From the Ionosphere," *Royal Society of London Proceeding Series A*, vol 227, pp 516-537, 1955.

2-2 Wait, J.R., *Electromagnetic Waves in Stratified Media*, Pergamon Press, The MacMillan Company, New York, 1962.

2-3 Sheddy, C.H., Y. Gaugh, and R. Pappert, *An Improved Computer Program for VLF Mode Constants in an Earth-Ionosphere Waveguide of Arbitrary Electron Density Distribution*, Interim Report No. 682, Naval Electronics Laboratory Center, San Diego, California, January 1968.

2-4 Sheddy, C.H., R. Pappert, Y. Gaugh, and W. Moler, *A Fortran Program for Mode Constants in an Earth-Ionosphere Waveguide*, Interim Report No. 683, Naval Electronics Laboratory Center, San Diego, California, May 1968.

2-5 Sheddy, C.H., "A General Analytic Solution for Reflection From a Sharply Bounded Anisotropic Ionosphere," *Radio Science*, vol 3, no.8, August 1968.

2-6 Booker, H.G., C.M. Crain, and E.C. Field, *A Panoramic View of Ionospheric Reflection and Transmission Under Ambient and Disturbed Conditions*, R-559-PR, Rand, Santa Monica, California, November 1970.

2-7 Wait, J.R., and L.C. Walters, "Reflection of VLF Radio Waves from an Inhomogeneous Ionosphere: Part 1, Exponentially Varying Isotropic Model," *Journal of Research, National Bureau of Standards*, 67D, no.3, pp 361-367, January 1963.

2-8 Gambill, B., and R. Rutherford, *WEDCOM Propagation Model Improvements*, 71TMP-27, General Electric—TEMPO, July 1971.

2-9. Field, E.C., and R.D. Engle, "Detection of Daytime Nuclear Bursts Below 150 km by Prompt Phase Anomalies," *Proceedings of the IEEE*, *53*, no.12, pp 2009-2017, 1965.

SECTION 3
WAVEGUIDE SOLUTIONS

INTRODUCTION

The ELF/VLF propagation models compute the received electric field strength as the summation of waveguide modes. Mode solutions are found for a uniform waveguide. In a strict sense, this solution is only applicable for ELF/VLF transmissions between a uniform concentric ionosphere and earth with a uniform magnetic field. In situations where the ionosphere is disturbed by nuclear detonations or where the propagation path crosses the sunset or sunrise terminator or a land-sea boundary, the waveguide is not uniform along the path.

Two procedures are used in WEDCOM to account for this nonuniformity. The first method is an approximation which assumes that the ionospheric or ground properties vary slowly in the direction of propagation. This method is called the WKB approximation. The second method models the nonuniform propagation path as several adjacent uniform waveguides with different propagation characteristics. An energy conversion process (mode conversion) is computed at each interface. The Mode Conversion method is used only for VLF cases. The WKB method is an option available for VLF cases and is used for all ELF cases.

The computational sequence requires defining uniform waveguide solutions (eigenvalues), using these to define values for attenuation rates and height gain and mode excitation factors, and applying these values in mode-summing equations to compute total field strength. The procedures are described in order below.

THE GENERAL MODE EQUATION

The general mode equation for a uniform waveguide can be written in the form

$$F(\theta) = (1 - {}_{\parallel}\bar{R}_{\parallel}{}_{\parallel}R_{\parallel})(1 - {}_{\perp}\bar{R}_{\perp}{}_{\perp}R_{\perp}) - {}_{\perp}R_{\parallel}{}_{\parallel}R_{\perp}{}_{\parallel}\bar{R}_{\parallel}{}_{\perp}\bar{R}_{\perp} \quad , \quad (3\text{-}1)$$

where ${}_{\parallel}R_{\parallel}$, ${}_{\perp}R_{\perp}$, ${}_{\perp}R_{\parallel}$, and ${}_{\parallel}R_{\perp}$ are the ionosphere reflection coefficients described in Section 2, and ${}_{\parallel}\bar{R}_{\parallel}$ and ${}_{\perp}\bar{R}_{\perp}$ are ground reflection coefficients for vertically and horizontally polarized waves. The mode equation requires that the R's and $\bar{R}$'s can be referenced to the same altitude. The R's are referenced to the bottom of the ionosphere, or to an altitude where most of the energy is reflected, or to ground, depending on the computational option used. Equations for the R's, referenced to a specified altitude, were taken from Reference 3-1 and adapted for use with Airy functions. The equations are described in detail in Appendix C.

VLF EIGENANGLE DETERMINATION

General

The eigenangles, θ_n, are those values for which $F(\theta)$ vanishes. They are difficult to determine explicitly and are found by iteration techniques. Determination of θ_n in WEDCOM is accomplished by two procedures. The first (identified here by A) is a search technique over the complex θ-plane, and is an adaptation of the MODESRCH algorithm (Reference 3-1). The second procedure (identified here by B) employs an analytic approximation of $F(\theta)$.

Both procedures use an analytic representation of the ionospheric reflection coefficients. This can be illustrated with the aid of Figure 3-1. Procedure A first identifies a set of rectangular regions of the θ-plane where the anisotropic ionospheric reflection coefficients are computed at each corner. A Lagrangian interpolation representation of the reflection coefficients is made for a rectangle followed by a search method to locate the eigenangles. For the purposes of WEDCOM, these approximate eigenangles have been found sufficiently accurate and iteration to the exact value is not performed as in the MODRSRCH program.

Procedure B computes the isotropic ionospheric reflection coefficients at two real θ values. An analytic formulation of the

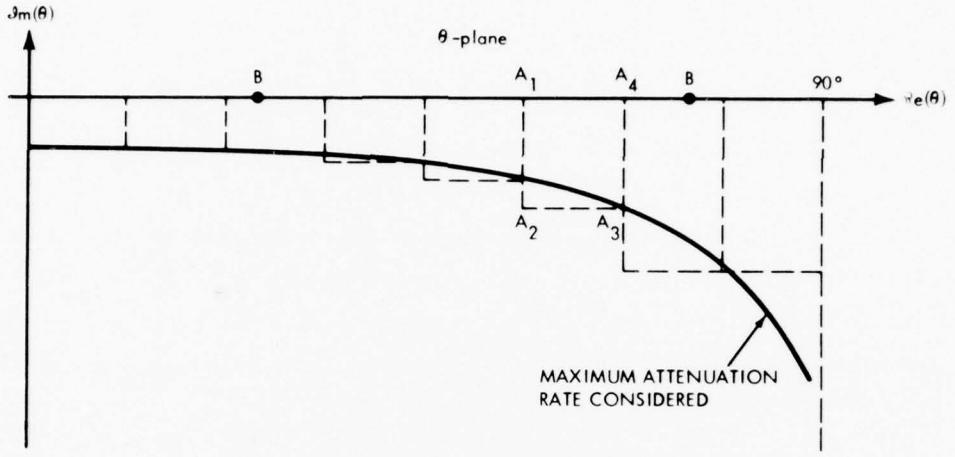

Figure 3-1. The complex θ-plane illustrating the θ values used in the ionospheric reflection coefficient computations for initial eigenangle determination.

reflection coefficients (using the two precomputed values) is employed to estimate approximate eigenangles. Next, a Newton-Raphson algorithm with these approximate eigenangles as initial values iterates to an exact eigenangle value using the anisotropic reflection coefficient model. This procedure is described in detail later in this section.

Procedure B is fast and accurate for daytime or strong nuclear-depressed ionospheres. The approximate eigenangles are sufficiently accurate for severely depressed ionospheres, and the exact eigenangle determination is not made. Procedure A utilizes more computation time, but is much more accurate for weakly disturbed nighttime ionospheric profiles. To help illustrate the weakness of Procedure B, Figure 3-2 shows the loci of eigenangles as a daytime profile is gradually changed to a nighttime profile. The eigenangles start at the left for the TE and TM modes, and progress as indicated by the arrow as the ionosphere is varied. For Procedure B, note that the

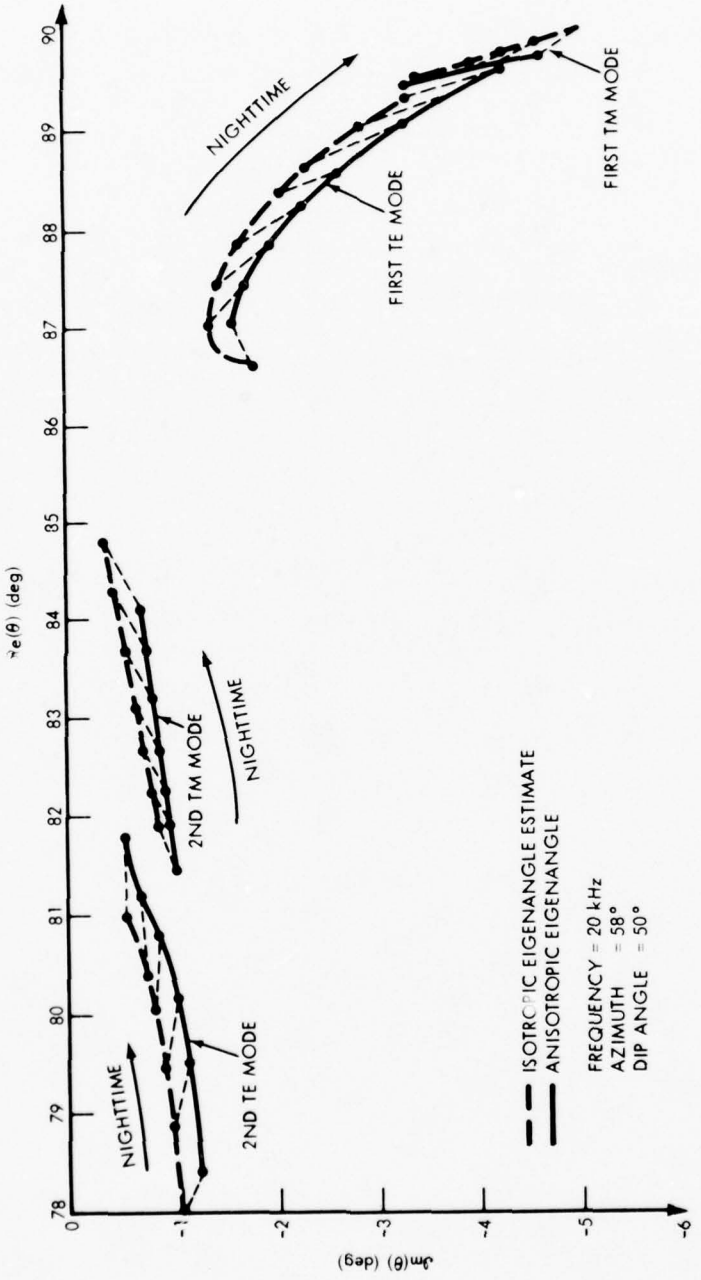

Figure 3-2. Loci of eigenangles.

isotropic solution provides an adequate approximation for the more depressed ionospheres, and convergence to the exact modes will occur with some confidence. However, as the nighttime profile is approached the eigenangles for the first TE and TM modes are nearly equal, and Procedure B will result in wrong convergence. The Search Method (Procedure A) works well for the nighttime cases, even those where the eigenangles are almost identical. Both procedures will now be described in more detail.

Search Procedure A

As mentioned above, this procedure is an adaptation of the MODESRCH techniques. A complete description is found in Reference 3-1, but the procedure is outlined here to assist in the description of the WEDCOM models (Volume 2). The search procedure is identical to all rectangles. Each rectangle is 5 degrees wide along the $Re(\theta)$ axis. The length along the $Im(\theta)$ axis is frequency dependent and is computed from a preselected maximum attenuation rate as a function of $Re(\theta)$ (see Figure 3-1).

The eigenangle θ_n search for very oblique ionospheric incidence is numerically difficult due to a pole in $F(\theta)$ at $\theta = 90°$, and another potential pole in the ground reflection coefficients, ${}_{\parallel}\bar{R}_{\parallel}$ and ${}_{\perp}\bar{R}_{\perp}$. Thus, the modal equation, $F(\theta)$, is modified by first defining

$$ {}_{\parallel}\bar{R}_{\parallel} = \frac{{}_{\parallel}N_{\parallel}}{{}_{\parallel}D_{\parallel}} \tag{3-2} $$

$$ {}_{\perp}\bar{R}_{\perp} = \frac{{}_{\perp}N_{\perp}}{{}_{\perp}D_{\perp}} \tag{3-3} $$

$$ {}_{\parallel}X_{\parallel} = \frac{({}_{\parallel}R_{\parallel} + 1)}{C} \tag{3-4} $$

$$ {}_{\perp}X_{\perp} = \frac{({}_{\perp}R_{\perp} + 1)}{C} \tag{3-5} $$

$$ {}_{\parallel}X_{\perp} = \frac{{}_{\parallel}R_{\perp}}{C} \tag{3-6} $$

$$ {}_{\perp}X_{\parallel} = \frac{{}_{\perp}R_{\parallel}}{C} \tag{3-7} $$

where C is the cosine of the angle of incidence, and ${}_{\parallel}N_{\parallel}$, ${}_{\parallel}D_{\parallel}$, ${}_{\perp}N_{\perp}$, and ${}_{\perp}D_{\perp}$ are defined with no poles in the region of interest. The pole at $\theta = 90°$ has been removed from the R's with the definition of the X's (Reference 3-2). A new modal equation is formulated with the substitution of Equations 3-2 through 3-7 into Equation 3-1 and rearranging:

$$ F_m(\theta) = \frac{{}_{\parallel}D_{\parallel}\ {}_{\perp}D_{\perp}}{C^2} F(\theta) \quad . \tag{3-8} $$

The modified modal equation $F_m(\theta)$ is analytic and presents little numerical difficulty for the θ region of interest.

The validity of the search procedure is premised on the Argument Principal of complex variable theory, which insures that the phase change of $F_m(\theta)$ will complete a cycle for each eigenangle when $F_m(\theta)$ is traced counterclockwise around the rectangle.

Figure 3-3 presents an enlargement of one of the rectangles of Figure 3-1. The finer mesh size is smaller than the separation of the eigenangles. Starting at the rectangle corner A_I and proceeding counterclockwise, the character of $F_m(\theta)$ is examined at each mesh corner. This investigation is based on the following definition of $F_m(\theta)$:

$$ F_m(\theta) = F_R + jF_I = |F_m| e^{j\phi_F} \quad . \tag{3-9} $$

Thus, when $F_m(\theta) = 0$, $F_R = F_I = 0$, and θ_m is undefined. Also note other $F_m(\theta)$ characteristics in Table 3-1. Thus, if F_I changes sign from one mesh corner to an adjacent corner, then the line $F_I = 0$ enters that mesh somewhere along the mesh edge. Thus, using the example illustrated in Figure 3-2, no F_I sign change would occur until mesh 3. The eigenangle search continues as follows:

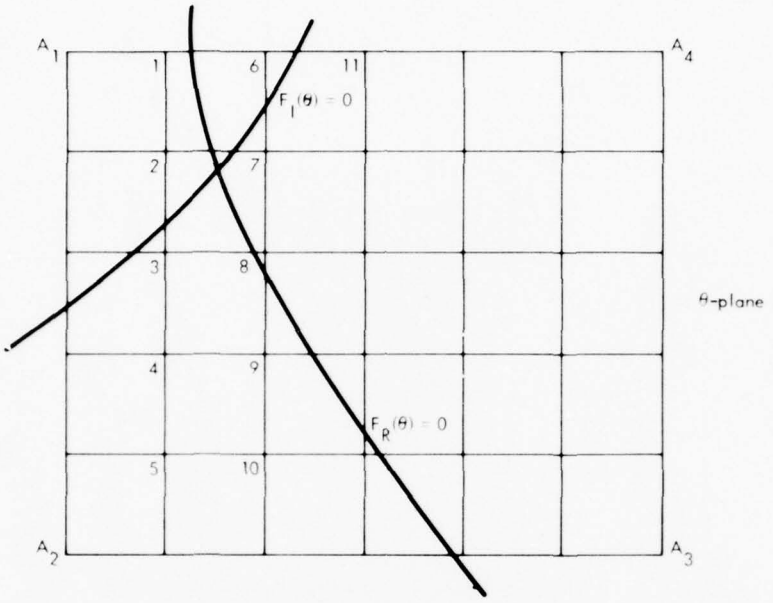

Figure 3-3. Illustrating the mesh squares of the contour rectangle $A_1A_2A_3A_4$ in Figure 3-1.

Table 3-1. Characteristics of $F_m(\theta)$.

F_R	F_I	ϕ_F
0	>0	90°
0	<0	-90°
>0	0	0°
<0	0	180°
0	0	Undefined

1. The mesh 3 edge where $F_I = 0$ exist is determined by computing F_I at the remaining two corners. A check is made to determine if possibly one other $F_I = 0$ curve may also enter and exit mesh 3 (all adjacent corners would have an opposite sign). Finally, F_R is computed at the four corners to see if an $F_R = 0$ line enters and exits mesh 3. These tests assume that F_I and F_R are linear with θ along the edges, and so only one $F_I = 0$ or $F_R = 0$ line crossing can occur along one edge.
2. The $F_I = 0$ line exits along the upper edge of mesh 3. Mesh 2 is examined as in step 1 followed by meshes 7, 6, and 11. The exit point from the rectangle is noted (mesh 11) so that reentry will not be performed as the search continues around the rectangle contour.
3. Lines of $F_I = 0$ and $F_R = 0$ were found in mesh 7. Again, assuming the linear behavior of F_I and F_R along the mesh edges, simple curves (Hyperbolic) are formed within the mesh. If the computed crossing lies along the $F_I = 0$ line being traced, an eigenangle is identified. The remaining rectangle is similarly searched, starting with mesh 4 and continuing until all four rectangle edges have been traced.

The eigenangles found are approximate, as the mesh employed a simple hyperbolic curve mesh geometry to determine the eigenangle location. A Newton-Raphson iteration procedure is used to remove this approximation. When two eigenangles are located very close, this procedure is modified to insure that the Newton-Raphson procedure does not iterate both approximations to the same eigenangle.

Isotropic Ionosphere Procedure B

Procedure B initially assumes an isotropic ionosphere, which is applicable when the earth's magnetic field is small and ${}_{\perp}R_{\parallel}$ and ${}_{\parallel}R_{\perp}$ are approximately zero. For this situation Equation 3-1 can be rewritten as

$$F(\theta) = (1 - {}_{\parallel}\bar{R}_{\parallel}R_{\parallel})(1 - {}_{\perp}\bar{R}_{\perp}R_{\perp}) \quad . \tag{3-10}$$

This permits independent solutions for vertical and horizontal polarization to be made; ie,

$$1 - {}_{\parallel}R_{\parallel}\bar{R}_{\parallel} = 0 \tag{3-11}$$

$$1 - {}_{\perp}R_{\perp}\bar{R}_{\perp} = 0 \quad . \tag{3-12}$$

For convenience in the following discussion, the definitions below are made:

$$r_i = \begin{cases} {}_{\parallel}R_{\parallel} & \text{when solutions for vertical polarization are sought} \\ {}_{\perp}R_{\perp} & \text{when solutions for horizontal polarization are sought} \end{cases} \tag{3-13}$$

$$r_g = \begin{cases} {}_{\parallel}\bar{R}_{\parallel} & \text{when solutions for vertical polarization are sought} \\ {}_{\perp}\bar{R}_{\perp} & \text{when solutions for horizontal polarization are sought} \end{cases} \tag{3-14}$$

Equations 3-11 and 3-12 can be written in terms of Airy functions as

$$A(t_n)\ B(t_n) = e^{-j2\pi n} \tag{3-15}$$

for the nth mode and where t_n is a uniquely determined eigenangle (Reference 3-2). The functions $A(t_n)$ and $B(t_n)$ are defined by

$$A(t_n) = -\frac{W_1'(t_n - y_R) + q_i W_1(t_n - y_R)}{W_2'(t_n - y_R) + q_i W_2(t_n - y_R)} \tag{3-16}$$

$$B(t_n) = -\frac{W_2'(t_n) - qW_2(t_n)}{W_1'(t_n) - qW_1(t_n)} \tag{3-17}$$

where $W_1(t)$ and $W_2(t)$ are Airy functions of the first and second kinds and the prime indicates the derivative with respect to the argument.

In Equations 3-16 and 3-17, q_i and q are the normalized impedance is defined by

$$q_i = \frac{-j(y_R - t_n)^{1/2}(1 - r_i)}{1 + r_i} \quad , \tag{3-18}$$

where

$$y_R = \frac{k}{k_a} z_R \tag{3-19}$$

z_R = reference altitude (km), defined by Equation 2-35
a = earth's radius (km)
k = wavenumber (km)
$k_a = (ka/2)^{1/3}$.

The normalized surface impedance at the ground is

$$q = \begin{cases} Q_H/n_g^2 & \text{vertical polarization} \\ -jk_a n_g & \text{horizontal polarization} \end{cases} \tag{3-20}$$

where

$$n_g^2 = \varepsilon - j\frac{\sigma}{\omega\varepsilon_o}$$

$$Q_H = jk_a(n_g^2 - S^2)^{1/2}$$

S = sine of the eigenangle at the ground
k = wavenumber (km^{-1})
ε = relative dielectric constant of the earth
σ = earth conductivity (mhos/m)
ε_o = permittivity of free space (farads/m) .

The above definitions coupled with the analytic approximations to the reflection coefficients (Equation 2-26) permit several approximations to Equation 3-15. Equation 3-15 can be approximated by (Reference 3-2)

$$e^{-j2\pi n} = r_i r_g F_g \exp -\left\{\left[j2k\ a/3\right]\left[(C')^3 - C^3\right]\right\} \quad , \quad (3\text{-}21)$$

where

$$C' = (y_R - t)^{1/2}/k_a \quad (3\text{-}22)$$

$$C = (-t)^{1/2}/k_a \quad . \quad (3\text{-}23)$$

C' is the complex cosine of the angle of incidence at the ionosphere, and C is the complex cosine of the angle of incidence at the ground. Also, C and C' are related by

$$C' = (C^2 + y_R/k_a^2)^{1/2} \quad . \quad (3\text{-}24)$$

F_g is a correction factor to account for errors in the approximation of B(t) and is discussed below.*

Using Equation 2-26, Equation 3-21 can be written for the nth mode as

$$2\pi n = \pi + j(\alpha_1 C' + j\alpha_2 C') - \alpha_3 (C') + \left[(C') - C^3\right]\left(\frac{2ka}{3}\right) + j\ \ell n\ (r_g) + j\ \ell n\ (F_g) \quad . \quad (3\text{-}25)$$

If r_g is represented by a Fresnel reflection coefficient, F_g can be expressed as

$$F_g = \frac{\dfrac{W_2'(t) - qW_2(t)}{W_1'(t) - qW_1(t)}}{j\ \exp\left[j4/3(-t)^{3/2}\right]\left(\dfrac{-j(-t)^{1/2} - q}{j(-t)^{1/2} - q}\right)} \quad (3\text{-}26)$$

*For simplification the subscript "n" has been omitted in this section for t_n. It will be understood that t refers to the nth mode for either vertical or horizontal polarization.

For vertical polarization, F_g varies rapidly with ground conductivity if the conductivity is less than 10^{-3} mho/m.

APPROXIMATIONS TO ISOTROPIC MODE EQUATION. To solve Equation 3-25, it is convenient to define the product F_{gr} as

$$F_{gr} = F_g r_g = \frac{j\dfrac{W_2'(t) - qW_2(t)}{W_1'(t) - qW_1(t)}}{\exp\left[j4/3(-t)^{3/2}\right]} \quad . \tag{3-27}$$

The procedure used to solve Equation 3-25 is as follows:

1. Assume that t lies between some limiting values for which an approximate form for the Airy function can be used.
2. Approximate F_{gr} by its value for highly conducting earth, and obtain a solution to Equation 3-25.
3. Test to see if the solution for t is in the assumed range. If not, assume another range and repeat Steps 1 and 2.
4. If the actual ground conductivity is less than 10^{-3} mho/m, F_{gr} is redefined by substituting the solution to Equation 3-21 from Step 2 and using a value of condictivity slightly less than 10^{-3} mho/m. This process is continued, reducing the conductivity each time, until the conductivity is reduced to the desired low value.

No iteration on conductivity is required for horizontal polarization, since the high-conductivity approximation applies for all reasonable values of ground conductivity. Approximate values for F_{gr} and the resulting solutions for Equation 3-25 for both vertical and horizontal polarization are given below.

Case 1a. $Re(-t) > 1$, vertical polarization.

This is the modified flat-earth approximation, which is better when used with waveguide upper boundaries typical of normal daytime or nuclear-disturbed ionospheres and for higher modes. For this case, $F_{gr} \approx 1$ and an approximate solution of Equation 3-25 is found by first obtaining C'' from

$$C'' = \frac{R_n\left[2kz_R - j\alpha_e\sqrt{1 + 4z_R^3k^2/(R_n^2a)}\right]}{4k^2z_R^2 + \alpha_e^2} \qquad (3\text{-}28)$$

and then using

$$C = \left[(C'')^2 - \frac{z_R}{a}\right]^{1/2} , \qquad (3\text{-}29)$$

where initially

$$\alpha_e = \alpha_1 + j\alpha_2 \qquad (3\text{-}30)$$

$$R_n = \pi(2n - 1) . \qquad (3\text{-}31)$$

Both α_e and R_n are varied in an iterative solution. α_e is modified to account for the second-order term in Equation 2-26, and R_n is modified to account for variation in F_{gr} with decreasing conductivity. In the iteration procedure, α_e and R_n are represented in subsequent steps in the iteration by

$$\alpha_e = \alpha_1 + j\alpha_2 + j\alpha_3\left[(C_p'')^2 + \frac{z_R}{a}\right]^{1/2} \qquad (3\text{-}32)$$

$$R_n = \pi(2n - 1) - j\,\ell n\, F_{gr}(C_p'', \sigma_p) , \qquad (3\text{-}33)$$

where σ_p and C_p'' are values from the previous iteration and $F_{gr}(C_p'', \sigma_p)$ is evaluated using Equation 3-27 with values of t and q determined by C_p'' and σ_p, respectively.

Case 1b. $Re(-t) > 1$, horizontal polarization.

The solution for horizontal polarization is

$$C'' = \frac{R_n\left[2kz_R - j\alpha_e\sqrt{1 + 4z_R^3k^2/(aR_n^2)}\right]}{4k^2z_R^2 + \alpha_e^2} , \qquad (3\text{-}34)$$

where $R_n = 2\pi n$ and is relatively independent of conductivity, and α_e is determined as described above.

Case 2a. $|t| < 1$, vertical polarization.

For waveguide upper boundaries determined by normal or weakly disturbed nighttime boundaries, a grazing-earth incident angle approximation is often applicable for lower mode numbers. If the magnitude of t is small and the conductivity is greater than about 10^{-3} mho/m,

$$F_{gr} \approx \exp(j\ /6)\ \exp\left[-j\,\frac{4}{3}(-t)^{3/2}\right] \quad . \tag{3-35}$$

Making the further approximation that

$$C^2 << \frac{2z_R}{a} \quad , \tag{3-36}$$

which should be true if t is small, the solution to Equation 3-25 can be written as

$$C^2 = \frac{R_n - \left(\frac{2ka}{3}\right)\left(\frac{2z_R}{a}\right)^{3/2} + (\alpha_2 - j\alpha_1)\left(\frac{2z_R}{a}\right)^{1/2} + \alpha_3\left(\frac{2z_R}{a}\right)}{k\left(\frac{2z_R}{a}\right)^{1/2} - \alpha_3 + \frac{j(\alpha_1 + i\alpha_2)}{2\left(\frac{2z_R}{a}\right)^{1/2}}} \quad . \tag{3-42}$$

R_n is defined by

$$R_n = \pi\frac{12n - 5}{6} - j\ \ell n\ F_{gr} \quad . \tag{3-38}$$

Initially, R_n is defined for high-conductivity ground and is subsequently modified in an iteration loop to account for low conductivity.

Case 2b. $|t| < 1$, horizontal polarization.

For these conditions,

$$F_{gr} \approx \exp\ (j5\pi/6)\ \exp\left[-j\,\frac{4}{3}(-t)^{3/2}\right] \quad . \tag{3-39}$$

The solution for C^2 is the same as for vertical polarization except that R_n is replaced by

$$R_n = \pi(12n - 1)/6 \tag{3-40}$$

and does not vary with conductivity.

Case 3a. $Re(t) > 1$, vertical polarization.

When the ionospheric reflection altitude is high, there results what is known as a "detached whispering gallery" mode. Here

$$F_{gr} \approx \exp(j\pi/2)\exp\left[-j\frac{4}{3}(-t)^{3/2}\right] \tag{3-41}$$

$$C^2 = X^2\left\{1 - X^2\frac{\frac{j(\alpha_1 + \alpha_2)}{2}\left(\frac{2z_R}{a}\right)^{-1} + ka}{4\left[ka\left(\frac{2z_R}{a}\right) - \alpha_3\left(\frac{2z_R}{a}\right)^{1/2} + \frac{j(\alpha_1 + j\alpha_2)}{2}\right]}\right\}$$

X^2 is equal to the value of C^2 that is obtained from Equation 3-37 but with R_n replaced by

$$R_n = \pi\left(\frac{4n - 1}{2}\right) \quad . \tag{3-43}$$

Case 3b. $Re(t) > 1$,

The same equations used for vertical polarization are used for this case.

ITERATION ALGORITHMS. Equation 3-15 is solved using Newton's iteration method. Given an initial guess, t_{n0}, an improved guess is obtained from

$$t_{n1} = t_{n0} + \Delta t \quad , \tag{3-44}$$

where

$$\Delta t = \frac{A(t_{n0})B(t_{n0}) - 1}{\frac{2j(t_{n0} - q^2\ (A(t_{n0})}{\left[W_1'(t_{n0}) - qW_1(t_{n0})\right]^2} + \frac{2j(q_i^2 - t_{n0} + y_o)B(t_{n0})}{\left[W_2'(t_{n0} - y_o) + q_i W_2(t_{n0} - y_o)\right]^2}} \tag{3-45}$$

An iteration procedure using Equations 3-44 and 3-45 and an initial guess from an appropriate approximation to Equation 3-25 is used to make Δt small. For Newton's method to converge to the appropriate value for a specified mode, a sufficiently good guess is required for t_{n0}.

A second iteration procedure is now used to obtain the exact eigenangles of Equation 3-1. The improved guess determined above is used with the Newton-Raphson and anisotropic ionospheric reflection coefficient algorithms. The procedure is to compute a correction term

$$\Delta\theta_n = -F(\theta) \Big/ \left.\frac{dF(\theta)}{d\theta}\right|_{\theta=\theta_o} , \tag{3-46}$$

where θ_o is the value for the present iteration. A new value is used defined using

$$\theta = \theta_o + \Delta\theta_n , \tag{3-47}$$

and Equation 3-46 is applied iteratively until $\Delta\theta_n$ becomes less than some preset criterion.

VLF FIELD STRENGTH EQUATIONS

The WEDCOM code provides two alternative procedures for computing the received electric field strength produced by an arbitrarily oriented transmitting dipole. The first method, the WKB approximation, assumes that the ionospheric profile and ground conductivity vary slowly as the signal propagates through the earth-ionosphere waveguide. As long as there are no abrupt transitions and the total transition is not severe, this first-order approximation is adequate and an easily

interpretable set of computations is provided. On the other hand, the WKB approximation becomes of questionable use when sharp changes in the ionosphere or ground characteristics occur. Implicit to the WKB approximation is that each mode can be traced as the signal propagates along the waveguide. Note from the example of Figure 3-3 the difficulty of mode identification if there is a sharp transition from a daytime to a nighttime profile. In addition, a sharp transition would scatter energy from one incident mode into other modes, violating another WKB assumption that all the energy would remain in the same mode.

These problems do not occur with the second method, the Mode Conversion procedure. At a transition region, mode identification need not occur for this procedure, and energy scattering into other modes is considered. Except for special cases, however, the mode conversion computations are not as easily interpretable as is the WKB method.

Both procedures segment the waveguide into N_p cascaded, uniform waveguides where the propagation characteristics do not change in any segment. Thus, the eigenangle computations defined earlier are applicable for either technique. Before proceding to a detailed description of these procedures, the WEDCOM transmitted power input options will be discussed. The input quantity is the effective free-space antenna input power. For a lossless short-wire antenna in free space, the input power and current moment are related by

$$P_{efs} = [3.5 \times 10^{-6} f I_m]^2 \quad \text{kW} \quad , \tag{3-48}$$

where

f = frequency (kHz)

I_m = current moment (ampere meters) .

However, it is the equivalent orthogonal (vertical, broadside, and endfire) dipole moments that are used in WEDCOM:

$$P_V = P_{efs} \cos^2\lambda$$

$$P_E = P_{efs} \sin^2\lambda \cos^2\phi \qquad (3\text{-}49)$$

$$P_B = P_{efs} \sin^2\lambda \sin^2\phi \quad ,$$

where (see Figure 1-1)

λ = dipole zenith angle (deg)

ϕ = angle between the x-axis and the dipole axis (deg) .

WKB Approximation

The WKB formulation used in WEDCOM is basically that described in Reference 3-3 and is repeated here for completeness. The three orthogonal dipole components defined above are considered a vertical component and two horizontal components, one aligned with the direction of propagation (endfire) and one at right angles to the direction of propagation (broadside). Three components of the electric field are computed: E_x, E_y, and E_z. The basic equations used for a nonuniform ionosphere for each mode are given below:

$$E_{\ell n} = Q_n \xi_{\ell n} g_{\ell n}^{N_p} \qquad V/m \quad , \qquad (3\text{-}50)$$

where n is the mode number, and

$$\ell = x, y, z \qquad (3\text{-}51)$$

$$\xi_{\ell n} = \left\{ P_V^{1/2} \lambda_{V\ell n} g_{zn}^1 + P_B^{1/2} \lambda_{B\ell n} g_{yn}^1 + P_E^{1/2} \lambda_{E\ell n} g_{xn}^1 \right\} \qquad (3\text{-}52)$$

$$Q_n = 0.05441 \left[\frac{f/a}{\sin (d/a)} \right]^{1/2} \exp [-jkd(\bar{S}_n - 1] \qquad (3\text{-}53)$$

f = frequency (kHz)

a = earth's radius (km)

d = path length (km)

k = wavenumber (km^{-1})

$\bar{S}_n$ = WKB approximation to the sine of the eigenangle, θ_n .

The λ's are representative excitation factors computed as a geometric mean:

$$\lambda_{ij} = (\lambda_{ij}^{1} \lambda_{ij}^{N_p})^{1/2} \quad . \tag{3-54}$$

The superscripts "1" and "N_p" indicate values at the transmitter and receiver, respectively. The g's are height-gain factors evaluated at the respective transmitter and receiver antenna altitudes. Both λ's and g's will be defined on the following pages.

To account for nonuniformities in ground and ionospheric parameters along the propagation path, two approximations are made. An average value is computed for the factor $\bar{S}_m$ in Equation 3-53. There are N_p computation points for a trunk, evenly spaced at distance d_R so that

$$\bar{S}_m = \left\{ \frac{\sin \theta_1 + \sin \theta_{N_p}}{2} + \sum_{i=2}^{N_p - 1} \sin \theta_i \right\} \frac{d_R}{d} \quad , \tag{3-55}$$

where θ_i is the eigenangle at the ith computation point.

The average attenuation rate and relative phase velocity are computed from

$$\bar{\alpha} = -8.69k \, Im(\bar{S}) \times 10^3 \text{ dB/Mm} \tag{3-56}$$

$$\frac{c}{v} = Re(\bar{S}) \quad , \tag{3-57}$$

where

c = velocity of light (km/s)

v = phase velocity (km/s) .

Mode Conversion Method

The WEDCOM mode conversion algorithm is an adaptation of the NOSC model (Reference 3-4). This model assumes that there is waveguide invariance normal to the waveguide, and that the reflections from the slab transitions may be neglected. This is consistent with Wait (Reference 3-5), who provides an argument demonstrating that neglect of reflections does not introduce much error. However, this

aspect should be explored further for very sharp transitional regions found in some nuclear environments.

The mode conversion algorithm formulation initially assumes that a unit amplitude wave exists in each mode in the transmitter slab. The quantities A^{p}_{jk} relate the energy from an incident mode k in the transmitter slab to the j^{th} mode in slab p. The mode conversion coefficients are computed by enforcing the boundary condition (at each slab interface) that all tangential field components must be continuous.

The three orthogonal electric field components E_{ℓ} (ℓ = x,y, and z) are computed. When the waveguide is uniform, the component computations are similar to the WKB solution; ie, for mode n

$$E_{\ell n} = Q_{n} \xi_{\ell n} g^{N_p}_{\ell n} \quad . \tag{3-58}$$

For the more general nonuniform waveguide case,

$$E_{\ell n} = \sum_{m=1}^{M^{N_p}} Q^{N_p}_{m,n} \; \xi_{\ell n} g^{N_p}_{\ell m} A^{N_p}_{mn} \quad , \tag{3-59}$$

where

$$Q^{N_p}_{m,n} = 0.05441 \left[\frac{f/a}{\sin(d/a)} \right]^{1/2} \exp \left[-jk \left\{ \sin(\theta^{1}_{n}) + \right. \right.$$

$$\left. \left. \sin(\theta^{N_p}_{m}) \; \frac{d_R}{2} - d \right\} \right] \tag{3-60}$$

$$d_R = \text{individual slab length (km)} \quad . \tag{3-61}$$

The mode conversion coefficient, $A^{N_p}_{mn}$, includes the effects of mode conversion and propagation in all slabs prior to the receiver slab.

Derivation of $A^{N_p}_{mn}$ is performed in Reference 3-6. The WEDCCM version is a simple extension of this derivation to consider cases where the number of eigenangles is not necessarily the same for all slabs. The mode conversion coefficients are determined by first solving for the parameter $a^{2}_{m,n}$ from

$$I^{2,1}_{\ell,n} = \sum_{m=1}^{M_2} a^{2}_{m,n}\, I^{2,2}_{\ell,m} \tag{3-62}$$

for the interface in the first two slabs, and solving for $a^{p+1}_{j,n}$ from

$$\sum_{m=1}^{M^2} a^{p}_{m,n}\, e^{-jk\,\sin(\theta^{p}_{m})d_R}\, I^{p+1,p}_{\ell,m} = \sum_{m=1}^{M^{p+1}} a^{p+1}_{m,n}\, I^{p+1,p+1}_{\ell,n} \tag{3-63}$$

for the remaining slab interfaces. The $I^{m,p}_{j,i}$ quantities are defined from

$$I^{m,p}_{j,i} = \begin{cases} \dfrac{\left[e^{p}_{i}(\delta e^{m}_{j}) - e^{m}_{j}(\delta e^{p}_{i}) + h^{p}_{i}(\delta h^{m}_{j}) - h^{m}_{j}(\delta h^{p}_{i})\right]_{0}^{z_R}}{kk_a\left[\sin(\theta^{m}_{j}) - \sin(\theta^{p}_{i})\right]} & \begin{array}{l} m \neq p \\ \text{and/or} \\ j \neq i \end{array} \\ \dfrac{2k_a\,\sin(\theta^{m}_{j})}{k}\left[(\delta e^{m}_{j})^2 + (\delta h^{m}_{j})^2 - t^{m}_{n}\left\{(e^{m}_{j})^2 + (h^{m}_{j})^2\right\}\right]_{0}^{z_R} & \begin{array}{l} m = p \\ \text{and} \\ j = i \end{array} \end{cases} \tag{3-64}$$

where z_R is the slab reflection altitude (Equation 2-35), and

$$e^{p}_{i} = \frac{F_3 W_2(t^{p}_{i}) - R_4 W_1(t^{p}_{i})}{F_3 W_2(t^{p}_{oi}) - F_4 W_1(t^{p}_{oi})} \tag{3-65}$$

$$\delta e^{m}_{j} = \frac{F_3 W'_2(t^{m}_{i}) - F_4 W'_1(t^{m}_{i})}{F_3 W_2(t^{p}_{oi}) - F_4 W_1(t^{p}_{oi})} \tag{3-66}$$

$$h^{p}_{i} = \frac{F_1 W_2(t^{p}_{i}) - F_2 W_1(t^{p}_{i})}{F_1 W_2(t^{p}_{oi}) - F_2 W_1(t^{p}_{oi})} \tag{3-67}$$

$$\delta h^{m}_{j} = \frac{F_1 W'_2(t^{m}_{j}) - F_2 W'_1(t^{m}_{j})}{F_1 W_2(t^{m}_{oj}) - F_2 W_1(t^{m}_{oj})} \tag{3-68}$$

$$t_{oi}^{p} = - \left[k_a \cos(\theta_i^p)\right]^2 \tag{3-69}$$

$$t_i^p = t_{oi}^p - kh/k_a \tag{3-70}$$

The W's are Airy functions and the F's will be defined in the next subsection. The $a_{m,n}^p$ are related to the mode conversion coefficients by

$$A_{m,n}^p = a_{m,n}^p \frac{\sin(\theta_m^p)}{\sin(\theta_n^2)} \tag{3-71}$$

The a_{jR}^2 and $a_{j,n}^{p+1}$ (right sides of Equations 3-62 and 3-63) are solved using Crout's L-V decomposition algorithm for the solution of simultaneous linear equations (Reference 3-7) of the form

$$[A]\bar{X} = \bar{B} \ . \tag{3-72}$$

The matrix [A] is or order (p-1) by (p-1), and $\bar{X}$ and $\bar{B}$ are (p-1) ordered vectors. As [A] and $\bar{B}$ are known, the vector $\bar{X}$ can be solved for. An improved estimate for $\bar{X}$ is obtained by first defining an error residue,

$$\bar{R} \equiv [A]\bar{X}_o - B \equiv [A]\bar{\delta X} \ . \tag{3-73}$$

A correction to $\bar{X}_o$ is made for $\bar{\delta X}$:

$$\bar{X} = \bar{X}_o - \bar{\delta X} \ . \tag{3-74}$$

This procedure is performed iteratively until $\bar{\delta X}$ becomes negligible.

The above procedure for computing $A_{m,n}^p$ is not used where the propagation characteristics between two slabs are almost identical. For this case,

$$A_{m,n}^p = A_{m,n}^{p-1} \, e^{-jk \sin(\theta_m^{p-1}) d_R} \ . \tag{3-75}$$

VLF Anistropic Excitation Factors

The λ's in Equation 3-52 are excitation factors, where the first subscript indicates the dipole component and the second subscript indicates the electric field component. They are computed from (References 3-8 and 3-9)

$$\lambda_{Vx} = \lambda_{Vz}/S$$

$$\lambda_{Vy} = -\frac{B}{S}\,{}_{\parallel}\bar{R}_{\perp}(1 + {}_{\parallel}R_{\parallel})(1 + {}_{\perp}\bar{R}_{\perp})$$

$$\lambda_{Vz} = B\,\frac{(1 + {}_{\parallel}\bar{R}_{\parallel})^2\,(1 - {}_{\perp}\bar{R}_{\perp}\,{}_{\perp}R_{\perp})}{{}_{\parallel}R_{\parallel}}$$

$$\lambda_{Ex} = -\lambda_{Vz}/S^2$$

$$\lambda_{Ey} = \frac{B}{S^2}\,{}_{\parallel}R_{\perp}(1 + {}_{\parallel}R_{\parallel})(1 + {}_{\perp}R_{\perp})$$

$$\lambda_{Ez} = -\lambda_{Vz}/S$$

$$\lambda_{Bx} = \lambda_{Bz}/S$$

$$\lambda_{By} = \frac{B}{S^2}\,\frac{(1 + {}_{\perp}\bar{R}_{\perp})^2(1 - {}_{\parallel}\bar{R}_{\parallel}\,{}_{\parallel}R_{\parallel})}{{}_{\perp}\bar{R}_{\perp}}$$

$$\lambda_{Bz} = -\frac{B}{S}\,{}_{\perp}R_{\parallel}(1 + {}_{\perp}R_{\perp})(1 + {}_{\parallel}\bar{R}_{\parallel}) \quad , \qquad (3\text{-}76)$$

where

$B = S^{5/2}/\partial F(\theta)/\partial\theta\,|\,\theta=\theta_n$

S = eigenangle ($\sin\theta_n$)

$F(\theta)$ = mode equation (see Equation 3-1) .

The R's are ionospheric reflection coefficients described in Section 2, and $\bar{R}$'s are ground reflection coefficients defined in Appendix C.

VLF Anisotropic Height Gain Factors

The g's in Equation 3-52 are height gain factors (Reference 3-8) and are computed from

$$g_x = \frac{1}{jk} \frac{g_z/a - e^{\left(\frac{z-z_{bot}}{a}\right)} \left[W_2'(t)F_1 - W_1'(t)F_2\right] k/k_a}{W_2(t_h)F_1 - W_1(t_h)F_2} \quad (3\text{-}77)$$

$$g_y = \frac{W_2(t)F_3 - W_1(t)F_4}{W_2(t_h)F_3 - W_1(t_h)F_4} \quad (3\text{-}78)$$

$$g_z = e^{\left(\frac{z-z_{bot}}{a}\right)} \frac{W_2(t)F_1 - W_1(t)F_2}{W_2(t_h)F_1 - W_1(t_h)F_2} \quad (3\text{-}79)$$

where

$$F_1 = W_1'(t_o) - QW_1(t_o) \quad (3\text{-}80)$$

$$F_2 = W_2'(t_o) - QW_2(t_o) \quad (3\text{-}81)$$

$$F_3 = W_1'(t_o) - Q_H W_1(t_o) \quad (3\text{-}82)$$

$$F_4 = W_2'(t_o) - Q_H W_2(t_o) \ . \quad (3\text{-}83)$$

z is the transmitter or receiver altitude (km), z_{bot} is the bottom of the ionosphere (ie, the altitude where the reflection coefficient integration is stopped), and the quantities Q and Q_H are defined in Appendix C.

The Airy function arguments t, t_o, and t_h are defined by

$$t = k_a^2(C^2 - 2(D - z)/a) \quad (3\text{-}84)$$

$$t_o = k_a^2(C^2 + \frac{2z}{a}) \quad (3\text{-}85)$$

$$t_h = -k_a^2(C^2 - 2(D - z_{bot})/a) \ , \quad (3\text{-}86)$$

where C is the cosine of the eigenangle, and D is the altitude where the modified index of refraction is unity. For the mode conversion computations D and z_{bot} are assumed to be zero.

VLF Isotropic Height Gain and Excitation Factors

When magnetic field effects are unimportant, the isotropic ionosphere approximation is used and the field equations are simplified. From Equation 3-76 when ${}_{\perp}R_{\parallel}$ and ${}_{\parallel}R_{\perp}$ are zero,

$$\lambda_{Vy} = \lambda_{Bz} = \lambda_{Ey} = 0 \tag{3-87}$$

The excitation and height gain factors required to compute the z and y components of the electric field are λ_{Vz}, λ_{Ez}, λ_{By}, g_x, g_y, and g_z. In the Airy function notation of Wait (Reference 3-2), they are

$$\lambda_{Vz} = -\lambda_{Ey} = A \frac{y_o}{2} \left\{ t - q^2 - \frac{\left(t - y_R - q_i^2\right)\left[W_2'(t) - qW_2(t)\right]^2}{\left[W_2'(t - y_R) + q_i W_2(t - y_R)\right]^2} \right\}^{-1} \tag{3-88}$$

where the q's and q_i's are evaluated for vertical polarization, and A is a constant. λ_{By} is evaluated from the same expression but with the q's and q_i's evaluated for horizontal polarization. In Equation 3-88 all ionospheric-dependent quantities are computed at the transmitter and receiver locations. To be applied directly in the electric field equations (Equations 3-52 or 3-55 and 3-56), the excitation factor defined by Equation 3-88 requires that

$$A = \frac{2}{kz_R} \quad . \tag{3-89}$$

The height gain factors are computed from

$$g_{z,y} = 0.5j \left\{ W_1(t - z)\left[W_2'(t) - qW_2(t)\right] - W_2(t - y_z) \times \left[W_1'(t) - qW_1(t)\right] \right\} , \tag{3-90}$$

where y_z is the normalized transmitter or receiver altitude:

$$y_z = \frac{kz}{k_a} \quad .$$

For vertical polarization $g_y = 0$ and, likewise, for horizontal polarization $g_z = 0$. Also, for vertical polarization,

$$g_x = g_z \frac{j}{k_a} \frac{W_2'(t - y_z) + B(t)W_1'(t - y_z)}{W_2(t - y_z) + B(t)W_1(t - y_z)} \tag{3-91}$$

SIGNAL-TO-NOISE RATIO CALCULATION

For the vertical electric field, the VLF signal-to-noise ratio in dB is

$$SNR = 20 \log_{10}(E_z/N_o) \tag{3-92}$$

$$N_o = 1.78 \times 10^{-14} B^{1/2} f \times 10^{(F_{am}/20)} , \tag{3-93}$$

where

f = frequency (khz)

B = bandwidth (Hz)

F_{am} = noise figure (dB above 273 × Boltzmann's constant).

F_{am} is defined in Reference 3-10, which also contains values for a grounded vertical dipole. The values are not valid for other polarizations.

ELF EIGENANGLE

Only one mode propagates at ELF, and it has been found that almost any reasonable initial estimate for the eigenangle will result in convergence. To compute the initial value, a typical eigenangle, θ_o, is first defined. A first-order improvement is made to this value as follows. The vertical ground reflection coefficient is assumed unity and the mode solution is approximated by

$$({}_nR_n - 1) \approx 0 . \tag{3-94}$$

Further, the assumption is made that

$${}_nR_n \approx e^{\alpha C + j\pi} , \tag{3-95}$$

where α is a complex constant. The reflection coefficient is computed using a typical incident angle θ_o. From Equations 3-94 and 3-95 it follows that the initial value, θ_i, can be found from

$$\theta_i = \cos^{-1}\left\{ - \frac{j\pi \cos\theta_o}{\ell n_{\mu} R_{\mu}\big|_{\theta=\theta_0}} \right\} . \qquad (3\text{-}96)$$

The exact value of the ELF eigenangle is determined by the Newton-Raphson iteration technique defined by Equations 3-46 and 3-47 using θ_i as an initial value.

ELF FIELD STRENGTH EQUATIONS

For transmitted field strength at ELF frequencies, the vertical E-field radiated from a surface horizontal dipole is computed. Since there is only one mode, the field is computed from

$$E_z = M \left(\lambda_{Bz}\, g_y^T + \lambda_{Ez}\, g_x^T \right) g_z^R \quad , \qquad (3\text{-}97)$$

where superscripts T and R refer to the transmitter and receiver locations respectively and the excitation factors are defined as they are for VLF cases, and the height gain factors are computed from

$$g_x = \frac{C\left(e^{jkCz} - {}_{\mu}\bar{R}_{\mu}\, e^{-jkCz} \right)}{1 + {}_{\mu}\bar{R}_{\mu}} \qquad (3\text{-}98)$$

$$g_y = \frac{e^{jkCz} + {}_{1}\bar{R}_{1}\, e^{-jkCz}}{1 + {}_{1}\bar{R}_{1}} \qquad (3\text{-}99)$$

$$g_z = \frac{e^{jkCz} + {}_{\mu}\bar{R}_{\mu}\, e^{-jkCz}}{1 + {}_{\mu}\bar{R}_{\mu}} \qquad (3\text{-}100)$$

These are flat-earth approximations which are valid at ELF where the ionospheric reflection coefficients are integrated to ground (ie, $z_{bot} = 0$).

The WKB procedure (described earlier for VLF field strength computations) is used for the ELF cases. The ionospheric ionization profile is analyzed at two additional locations (edges of Fresnel zone at midpath) to determine if the ionosphere is sufficiently uniform to assume the correctness of the WKB approximation. The WEDCOM output is flagged it if is determined that the WKB approximation might be invalid.

REFERENCES

3-1 Morfitt, D.G., and C.H. Shellman, *MODESRCH, An Improved Computer Program for Obtaining ELF/VLF/LF Mode Constants in an Earth-Ionosphere Waveguide*, Interim Report No. 77T, Naval Electronics Laboratory Center, San Diego, California, October 1976.

3-2 Wait, J.R., *Electromagnetic Waves in Stratified Media*, Pergammon Press, The MacMillan Company, 1962.

3-3 Pappert, R.A. and L.R. Shockey, *WKB Mode Summary Program for VLF/ELF Antennas of Arbitrary Length, Shape, and Elevation*, Interim Report No. 713, Naval Electronics Laboratory Center, San Diego, California, June 1971.

3-4 Pappert, R.A., and L.R. Shockey, *Simplified VLF/LF Mode Conversion Program with Allowance for Elevated, Arbitrarily Oriented Electric Dipole Antennas*, Interim Report 771, Naval Electronics Laboratory Center, San Diego, California, October 1976.

3-5 Wait, J.R., "Mode Conversion and Refraction Effects in the Earth-Ionosphere Waveguide for VLF Radio Waves," J. Geophysical Research, 73 (11), 1978.

3-6 Pappert, R.A. and L.R. Shockey, *A Simplified Mode Conversion Program for VLF Propagation in the Earth-Ionosphere Waveguide*, Interim Report No. 751, Naval Electronics Laboratory Center, San Diego, California, October 1974.

3-7 Ralson, A. and H.S. Wilf, *Mathematical Methods for Digital Computers*, vol II, John Wiley and Sons, Inc., 1967.

3-8 Pappert, R.A., *On the Problems of Horizontal Dipole Excitation of the Earth-Ionosphere Waveguide*, Naval Electronics Laboratory Center, Interim Report No. 682, San Diego, California, April 1968.

3-9 Budden, J.G., "The Influence of the Earth's Magnetic Field on Radio Propagation by Waveguide Modes," Proc. Roy. Soc. (London), Series A 265, no. 1323, pp 538-553, 1962.

3-10 *World Distribution and Characteristics of Atmospheric Radio Noise*, CCIR Report 322, International Telecommunication Union, 1964.

SECTION 4
SKYWAVE AND GROUNDWAVE CALCULATIONS FOR LF

INTRODUCTION

In the LF program, computations are performed for the E_z (vertical), E_y (perpendicular), and E_x (end) field components. When an arbitrarily oriented dipole antenna is used, all three orthogonal components from each of the three orthogonal dipole moments are summed.

The LF propagation model uses ray theory with correction terms for diffraction around the surface of the earth. The ray geometry is adjusted for a nonuniform ionospheric disturbance. Elevated antennas are modeled, but a built-in model simplification (used to increase computation efficiency) is not applicable for antenna altitudes higher than aircraft altitudes (ie, 6-8 km).

LF FIELD STRENGTH EQUATIONS

The total field strength for signals propagated at LF is represented as the sum of a groundwave and a number of skywaves. Specifically,

$$E_z = E_{gz} + \sum_{m=1}^{M} E_{z,m} \tag{4-1}$$

$$E_y = E_{gy} + \sum_{m=1}^{M} E_{y,m} \tag{4-2}$$

$$E_x = \sum_{m=1}^{m} E_{x,m} \quad , \tag{4-3}$$

where

E_z = total vertical field strength (V/m)

E_y = total field strength perpendicular to direction of propagation (V/m)

E_x = total field strength in direction of propagation (V/m)

E_{gz} = vertical component of groundwave (V/m)

E_{gy} = horizontal component of groundwave (V/m)

$E_{z,m}$ = vertical field strength for skywave with m ionospheric reflections (V/m)

$E_{y,m}$ = perpendicular field strength for a skywave with m ionospheric reflections (V/m)

$E_{x,m}$ = end field strength for a skywave with m ionospheric reflections (V/m).

When the ionosphere is anisotropic, the skywaves for vertical and horizontal polarization are coupled. This point will be discussed in detail later.

Radiated Power

The fields are formulated in terms of radiated power. In the computer model the effective free-space lossless dipole antenna input power, P_{efs}, is specified. The three orthogonal (vertical, broadside, and endfire) dipole powers are used in the LF model computations:

$$P_V = P_{efs} \cos^2\lambda \tag{4-4}$$

$$P_B = P_{efs} \sin^2\lambda \cos^2\phi \tag{4-5}$$

$$P_E = P_{efs} \sin^2\lambda \cos^2\phi \quad , \tag{4-6}$$

where (see Figure 1-1)

λ = dipole zenith angle (deg)

ϕ = angle between the X-axis and dipole axis (deg).

Groundwave Field

The groundwave field is given by (References 4-1 and 4-2)

$$E_{zg} = \frac{0.3P_V^{1/2}W_z}{d} \text{ V/m} \qquad \text{(vertical dipole)} \tag{4-7}$$

$$+ \frac{0.3P_E^{1/2}W_z}{dn_g} \text{ V/m} \qquad \text{(horizontal dipole endfire)} \qquad (4\text{-}8)$$

$$E_{yg} = \frac{0.3P_B^{1/2}W_y}{d} \text{ V/m} , \qquad \text{(horizontal dipole broadside)} \qquad (4\text{-}9)$$

where

$$n_g = \left(\frac{\sigma_g + j\varepsilon_g\varepsilon_o\omega}{\varepsilon_o\omega} \right)^{1/2}$$

σ_g = conductivity at transmitter (mhos/m)

ε_g = relative dielectric constant at transmitter

ε_o = permittivity of free space (farads/m)

ω = wave frequency (radians/s)

$j = \sqrt{-1}$,

and where d is the transmitter-receiver separation distance in kilometers.

The loss functions W_z and W_y are defined by (Reference 4-2)

$$W_z = \left(\frac{\pi X}{j}\right)^{1/2} \sum_{s=1}^{\infty} \frac{e^{-jXt_s}}{t_s - Q_z^2} \frac{W_1(t_s - y_1)}{W_1(t_s)} \frac{W_1(t_s - y_2)}{W_1(t_s)} \qquad (4\text{-}10)$$

and W_y is expressed the same way, except that Q_z is replaced by Q_y in Equation 4-10 and

$$X = \left(\frac{ka_e}{2}\right)^{1/3}\left(\frac{d}{a_e}\right) , \qquad (4\text{-}11)$$

where

k = wavenumber (km^{-1})

a_e = equivalent earth's radius (km)

and t_s (related to the eigenangle) is defined below.

In the LF calculations, a_e is defined as 4/3 the actual earth radius to correct for tropospheric refraction. The Q's are defined by

$$Q_z = -j \left(\frac{ka_e}{2}\right)^{1/3} \left(\frac{j\varepsilon_o\omega}{\bar{\sigma}_g + j\bar{\varepsilon}_g\varepsilon_o\omega}\right)^{1/2} \tag{4-12}$$

$$Q_y = -j \left(\frac{ka_e}{2}\right)^{1/3} \left(\frac{\bar{\sigma}_g + j\bar{\varepsilon}_g\varepsilon_o\omega}{j\varepsilon_o\omega}\right)^{1/2} , \tag{4-13}$$

where $\bar{\sigma}_g$ and $\bar{\varepsilon}_g$ are average conductivity and relative dielectric constant values over the entire path.

W_1 is the Airy function of the first kind (Reference 4-3). The arguments y_1, y_2 are defined by

$$y_1 = \left(\frac{2}{ka_e}\right)^{1/3} kh_{tr} \tag{4-14}$$

$$y_2 = \left(\frac{2}{ka_e}\right)^{1/3} kh_{rc} \tag{4-15}$$

where h_{tr} and h_{rc} are transmitter and receiver antenna heights in kilometers. The values of t_s are roots of the differential equation (Reference 4-1)

$$\frac{dt_s}{dq} = f(q,t_s) = \frac{1}{t_s - q^2} \tag{4-16}$$

and q is either Q_z (for E_z) or Q_y (for E_y).

The values of t_s are found by integrating the differential Equation 4-16 with respect to q using a fourth-order Runge-Kutta integration technique. Solutions for the starting condition (q=0) are known.

When Q (Q_z or Q_y) is small (less than one), the integration is performed by integrating Equation 4-16 from 0 to Q using as a starting value

$$t_s(q=0) = Z_s e^{-j\pi/3} , \tag{4-17}$$

where Z_s is the sth zero of $A_i'(-Z)$. The quantity $A_i'(-Z)$ is the conventionally defined Airy function (Reference 4-4). The first 10 zeros are shown in Table 4-1. When more than 10 terms are required in the integration, higher order zeros are computed from (Reference 4-4)

$$Z_s = -(y_s)^{2/3}\left[1 + \frac{7}{48y_s^2} + \frac{35}{288y_s^4} - \frac{181223}{207360y_s^6} + \frac{18683371}{1244160y_s^8}\right] \tag{4-18}$$

and

$$y_s = \frac{3\pi}{8}(4s - 3) \ . \tag{4-19}$$

After defining the initial values of t_s, the integration is performed using

$$t_s(q_{j+1}) = t_s(q_j) + \frac{1}{6}(P_1 + 2P_2 + 2P_3 + P_4) \ , \tag{4-20}$$

Table 4-1. Zeros of $A_i(-\alpha)$ and $A_i'(-\alpha)$.

Sequence Number	α_s = Zero of $A_i(-\alpha)$	α_s' = Zero of $A_i'(-\alpha)$
1	-2.33810741	-1.01879297
2	-4.08794944	-3.24819758
3	-5.52055983	-4.82009921
4	-6.78670809	-6.16330736
5	-7.94413359	-7.37217726
6	-9.02265805	-8.48848673
7	-10.04617434	-9.53544905
8	-11.00852430	-10.52766040
9	-11.93601556	-11.47505663
10	-12.82877675	-12.38478837

where

$$\Delta q = q_{j+1} - q_j \tag{4-21}$$

$$P_1 = f[q_j, t_s(q_j)]\Delta q \tag{4-22}$$

$$P_2 = f[q_j + 1/2\Delta q, t_s(q_j) + 1/2P_1]\Delta q \tag{4-23}$$

$$P_3 = f[q_j + 1/2\Delta q,\ t_s(q_j) + 1/2P]\Delta q \tag{4-24}$$

$$P_4 = f[q_j + \Delta q,\ t_s(q_j) + P_3]\Delta q \quad . \tag{4-25}$$

The solution is started using

$$f(0,t) = \frac{1}{t_s(0)} \quad . \tag{4-26}$$

Solutions for t_s are found using Equations 4-16 through 4-26 followed by defining the sth term in the summation in Equation 4-10. Terms are defined until the last term is less than 10^{-8}.

For vertical polarization and very low ground conductivity or for horizontal polarization in all cases, Q (ie Q_z or Q_y) becomes large. The procedure for determining t_s is similar to that used for small values of Q. The substitution

$$P = \frac{1}{Q} \tag{4-27}$$

is made in Equation 4-16, resulting in

$$\frac{dt_s}{dp} = \frac{1}{1 - t_s p^2} \quad . \tag{4-28}$$

The integration is performed by taking steps in Δp instead of Δq in Equation 4-19, and the starting values for p=0 are now defined by

$$t_s(p=0) = \alpha_s\, e^{-j\pi/3} \quad , \tag{4-29}$$

where the α_s's are the zeros of $A_i(-\alpha)$. The first 10 zeros are given in Table 4-1. When more terms are needed, higher order zeros are defined by (Reference 4-4)

$$\alpha_s = -(V_s)^{2/3}\left[1 + \frac{5}{48V_s^2} - \frac{5}{36V_s^4} + \frac{77125}{82944V_s^6} - \frac{108056875}{6967296V_s^8}\right] \tag{4-30}$$

and

$$V_s = \frac{3\pi}{8}(4s - 1) \quad . \tag{4-31}$$

Skywave Field Strength

The total skywave field strength is computed as the sum of field strengths of up to five skywaves. Figure 4-1 shows the geometric idealizations used in performing the skywave calculations. The rays bounce back and forth between the earth and an idealized sharply bounded ionosphere. The ionospheric boundary is defined at the altitude, h_R, that is in the center of a region in the ionosphere where most energy is reflected (see Equation 4-44b for the definition of h_R).

Path 1 in Figure 4-1 shows a case where the receiver is beyond the geometric horizon for a one-hop path. In this instance the ray is assumed to graze the earth's surface, and energy propagates the remaining distance by diffraction around the curved earth. This situation is referred to as propagation beyond the caustic. In the idealization used here, the diffracted distance, D_d, is assumed to be uniformly divided between transmitter and receiver ends.

Paths 2 and 3 illustrate ray paths that are within the geometric limit and show the geometry for a nonuniform ionosphere. The angle and distance quantities identified on the figure are used later in the discussion of the iteration procedures that define the geometry.

Fields for skywaves with N, N + 1, and N + 2 ionospheric reflections are always calculated, where N is the minimum number of skywave hops required to traverse the path without diffract around the earth's curvature are also considered. If N is 3 or greater, skywaves with N - 1 and N - 2 hops are considered. If N is 2, the field for a skywave with one hop is computed.

The general equations for describing the skywave field strengths are given first. Then the procedures defining the skywave geometry and the various parameters that are used in the general equations are provided.

GENERAL FIELD EQUATIONS. Because the model is developed to perform calculations when the ionosphere is nonuniform and anisotropic, the equations defining the multihop field strengths are cumbersome.

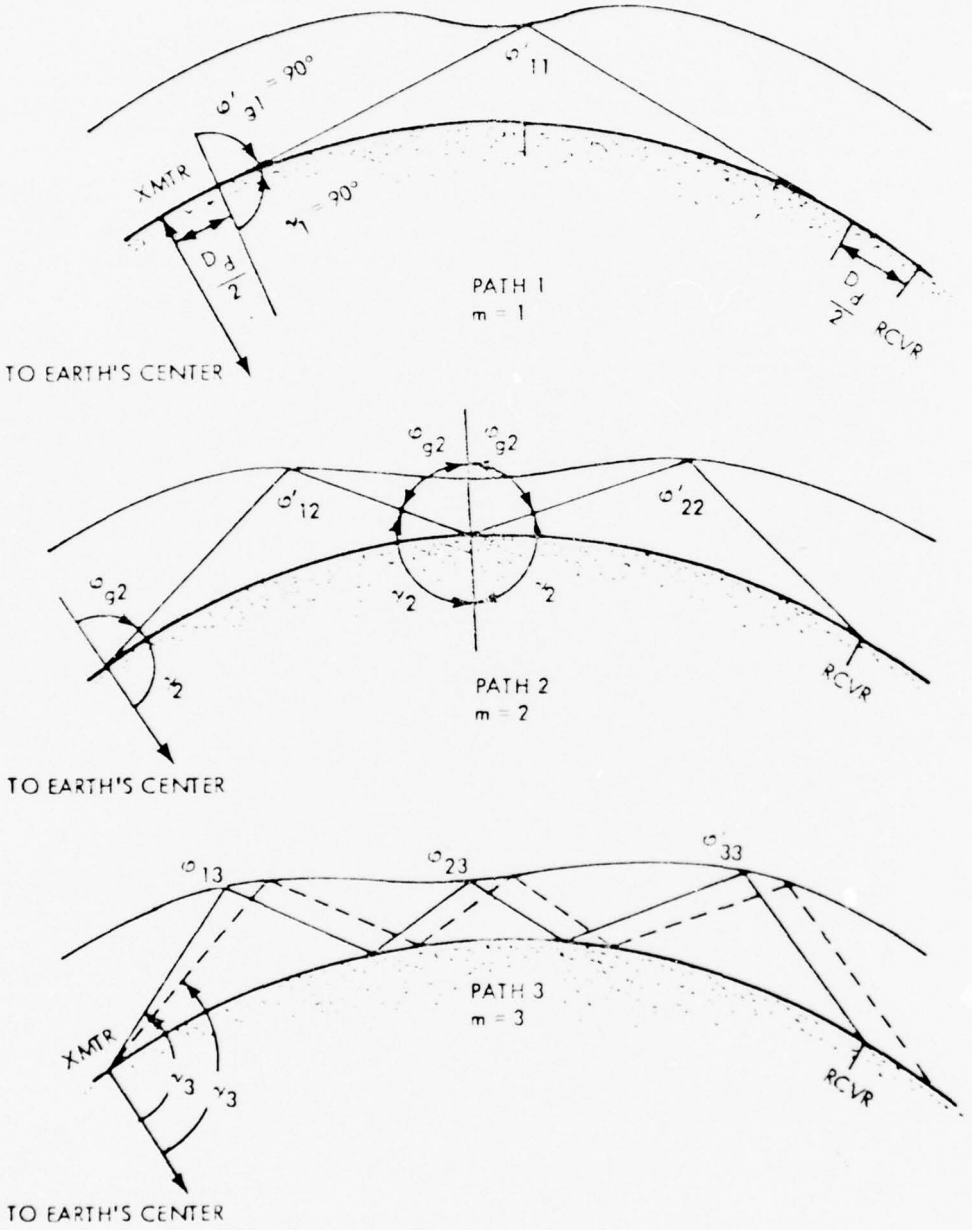

Figure 4-1. Ray geometry for nonuniform disturbance.

The following general nomenclature is used to simplify writing the equations:

		Polarization
R_{ij}^{VV}	Ionospheric reflection coefficient for the *ith* hop of a *j*-hop path	vertical to vertical
R_{ij}^{HV}	"	horizontal to vertical
R_{ij}^{VH}	"	vertical to horizontal
R_{ij}^{HH}	"	horizontal to horizontal
F_{Tj}^{VV}	Antenna foreground factor at the transmitter for a j-hop path	vertical field, vertical dipole
F_{Tj}^{HB}	"	horizontal field, broadside dipole
F_{Tj}^{VE}	"	vertical field, endfire dipole
F_{Rj}^{VV}	Antenna foreground factor at the receiver for a j-hop path	vertical field, vertical dipole
F_{Rj}^{HB}	"	horizontal field, broadside dipole
F_{Rj}^{VE}	"	vertical field, endfire dipole
G_{ij}^{V}	Ground reflection coefficient of diffractive correction factor for the ith hop of a j-hop path	vertical
G_{ij}^{H}	"	horizontal
E_{zj}	Vertical field for a j-hop skywave	
E_{yj}	Horizontal field for a j-hop skywave	
α_j	Convergence coefficient for a j-hop skywave	

Inverse distance field constants that account for the radiated power and total path distance are first computed. These are

$$E_{zo} = \frac{0.15P_V^{1/2}}{d} \text{ (vertical), or } \frac{0.15P_E^{1/2}}{d} \text{ (endfire)} \quad (4\text{-}32)$$

$$E_{yo} = \frac{0.15P_B^{1/2}}{d} , \quad (4\text{-}33)$$

where P_V, P_E, P_B, and d are as defined previously.

The field for a one-hop skywave is computed by first computing the intermediate quantity

$$I_{z1} = E_{zo}R_{11}^{VV}F_{T1}^{VX} + E_{yo}R_{11}^{HV}F_{T1}^{HB} \quad (4\text{-}34)$$

$$I_{y1} = E_{yo}R_{11}^{HH}F_{T1}^{HB} + E_{zo}R_{11}^{VH}F_{T1}^{VX} , \quad (4\text{-}35)$$

where $X \equiv V$ for a vertical dipole or $X \equiv E$ for an endfire horizontal dipole.

Then the field is computed from

$$E_{z1} = I_{z1}F_{R1}^{VX}\alpha_1 \quad (4\text{-}36)$$

$$E_{y1} = I_{y1}F_{R1}^{HB}\alpha_1 . \quad (4\text{-}37)$$

The field for a two-hop skywave is computed by first computing the intermediate quantity:

$$I_{z1} = E_{zo}R_{12}^{VV}F_{T2}^{VX} + E_{yo}R_{12}^{HV}F_{T2}^{HB} \quad (4\text{-}38)$$

$$I_{y1} = E_{yo}R_{12}^{HH}F_{T2}^{HB} + E_{zo}R_{12}^{VH}F_{T2}^{VX} . \quad (4\text{-}39)$$

Then

$$I_{z2} = I_{z1}R_{22}^{VV}G_{12}^{V} + I_{y1}R_{22}^{HV}G_{12}^{H} \quad (4\text{-}40)$$

$$I_{y2} = I_{y1}R_{12}^{HH}G_{12}^{H} + I_{z1}R_{22}^{VH}G_{12}^{V} \quad (4\text{-}41)$$

and

$$E_{z2} = I_{z2}F_{R2}^{VX}\alpha_2 . \quad (4\text{-}42)$$

$$E_{y2} = I_{y2} F_{R2}^{HB} \alpha_2 \tag{4-43}$$

The field for a greater number of hops is computed by a continuation of the process described above.

A vector sum and rms field sum are computed. The vector sum is obtained from

$$E_{zT} = E_{zg} + \sum_{n=L}^{n=N+2} E_{zn} \quad V/m \quad , \tag{4-44}$$

$$\bar{E}_{zT} = \left(E_{zg}^2 + \sum_{n=L}^{n=N+2} E_{zn}^2 \right)^{1/2} \quad V/m \quad . \tag{4-45}$$

In Equations 4-44 and 4-45, L is the maximum of 1 and N - 2.

The rms sum is computed because of uncertainty in the absolute phase of each skywave in a disturbed ionosphere, and because the prediction of deep nulls or high peaks in field strength calculations for a single path distance may be misleading. WEDCOM outputs the rms quantities when the field strength is to be computed only at the receiver. The vector sum is output when the field strength is computed at intermediate points along the path.

ELEVATED ANTENNA CONSIDERATIONS. When elevated antennas are used, up to four paths are considered for each number of hops as illustrated in Figure 4-2. The field strengths resulting from propagation via paths a_1, a_2, a_1, and b_2 are added vectorially to obtain a composite field strength for the particular skywave. The special definition of the antenna foreground factors for the case with elevated antennas is discussed later in this section. The four paths shown in Figure 4-2 are sufficient to define propagation for elevated antennas at less than 6-7 km. For higher altitudes, four more individual paths need to be considered.

INTERMEDIATE CALCULATIONS. The skywave geometry, ionospheric reflection coefficients, convergence coefficients, foreground factors, and ground reflection coefficients or diffraction loss factors are

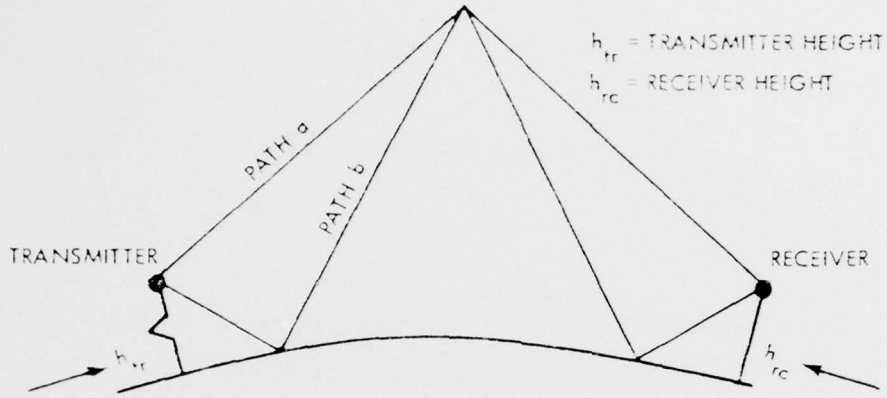

Figure 4-2. Geometry for four paths for elevated transmitters or receivers.

computed by performing the following sequential steps:

1. Search procedure for defining the skywave geometry and locating the ionospheric and ground reflection points.
2. Interpolation procedure for defining ionospheric and ground electrical properties at the reflection points.
3. Computation of ionospheric reflection coefficients.
4. Computation of convergence coefficients.
5. Computation of ground reflection coefficients or terms defining diffractive losses around the earth's bulge and antenna foreground factors.

Each of these steps is described below:

Search for Reflection Points. Reflection coefficients and reflection points (altitude and position along path) are determined for skywaves with m hops. Skywaves with m less than N (where N is the minimum number of hops needed to reach the receiver with no diffraction) are assumed to diffract over part of the path. An example is shown in Figure 4-1, where the skywave with one reflection (path 1) is assumed to propagate with one maximum-distance hop (grazing incidence at the earth) over part of the distance between transmitter and receiver and to propagate the remaining distance (D_d) by diffraction. In the example shown, two hops are the minimum number of hops that will reach from transmitter to receiver with no diffraction. Ground-based transmitters and receivers are shown in the example for simplicity. Modifications to account for elevated antennas are given later.

The steps in locating the reflection points are as follows:

1. A reference altitude and an ionospheric scale height are determined at specified intervals between transmitter and receiver. The reference altitude and ionospheric scale height are described below under Interpolation Procedure.

2. Skywaves with less than N hops are assumed to have grazing incidence (ϕ_g = 90 degrees). The distance between transmitter and receiver is divided into m equal intervals, and the reflection point of each hop is assumed to occur at the center of each interval. A trial reflection altitude for each hop, h_t, is picked (a starting value lower than the expected reflection altitude), and the angle of incidence with the ionosphere, ϕ_{it}, is computed. By interpolation between values calculated at the specified intervals, the actual reflection altitude, h_a, is found. If h_a is greater than h_t, then h_t is increased and the process is repeated until h_t is approximately equal to h_a.

3. For the ray path with N hops, a trial angle γ is calculated, and ionosphere reflection points and ground reflection points are found. The angle γ is then varied until the Nth ground reflection point coincides with the receiver. In carrying out this process, it is assumed that all ground reflection angles are equal to the take-off angle; however, the reflection altitude and hop distance may be different for each hop.

4. Step 3 is repeated for N + 1 and N + 2 hops to define the remaining ray paths. The dashed line for path 3 in Figure 4-1 shows one step in the interactive process in which γ is varied to find the location of the reflection points with three hops that reach the receiver.

Interpolation Procedure. Ionospheric parameters are evaluated at the trial reflection point by an interpolation procedure. The variables used in the interpolation procedure are shown in Figure 4-3. Ionospheric parameters are known at distances d_1 and d_2 that bracket the trial distance d_t. A linear interpolation procedure is used to define electron and positive ion vertical profiles at the distance d_t.

The ionospheric parameters used in the interpolation procedure are a reference altitude and an ionospheric scale height. Both are defined in terms of B(h), the imaginary part of the ionospheric index of reflection. The ionospheric scale height, h_s, is defined by

$$h_s = B(h) / \frac{d}{dh} \left[B(h) \right] . \tag{4-46}$$

The reference altitude h_R is defined by determining the altitude for which

$$B(h_R) = 0.04 . \tag{4-47}$$

The reference altitude h_R and scale heights h_s are obtained at distance d_t by linear interpolation between the values at d_1 and d_2.

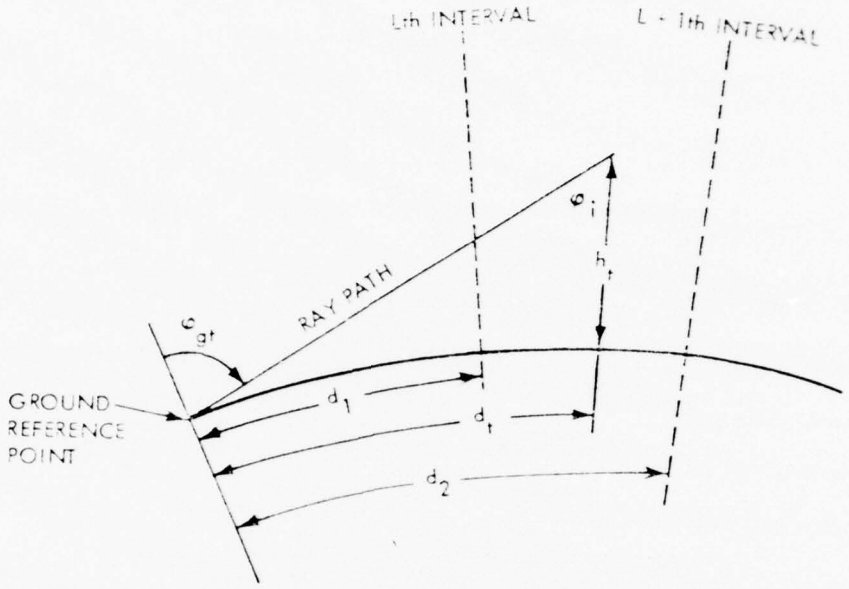

Figure 4-3. Variables in interpolation procedure.

The actual reflection altitude, h_r, is then estimated from

$$B(h_r) = \sqrt{2} \cos^2 \phi_i \ , \tag{4-48}$$

where ϕ_i is the ionospheric angle of incidence shown in Figure 4-3. Using Equation 4-45 and the definition of h_R and h_s results in

$$h_r = h_R \ell n \frac{\sqrt{2} \cos^2 \phi_i}{0.04} \tag{4-49}$$

The ionospheric region centered about the altitude h_r defined by Equation 4-49 has been shown to be the region from which most VLF and LF energy is reflected. Strictly speaking, it is applicable for an isotropic ionosphere and therefore for daytime or disturbed conditions. However, because of the steep vertical gradient of the ionospheric profile for normal nighttime conditions, the reflection

altitude is not sensitive to the criterion used, and therefore Equation 4-49 is used for all conditions.

When elevated antennas are used, four ray paths are considered as shown in Figure 4-4. In the iteration procedure, the great-circle distance covered by each ray path is

$$d_{a1} = D_{a1} - T_{a1} - R_{a1} \tag{4-50}$$

$$d_{a2} = D_{a2} + T_{a2} - R_{a2} \tag{4-51}$$

$$d_{b1} = D_{b1} + T_{b1} + R_{b1} \tag{4-52}$$

$$d_{b2} = D_{b2} - T_{b2} + R_{b2} \ . \tag{4-53}$$

In all cases (x is either a or b),

$$D_{xj} = a_e\left(\pi/2 - \gamma_{xj} - \psi_{xj}\right) \ , \tag{4-54}$$

$$T_{xj} = a_e \left(\pi/2 - \gamma_{xj} - \psi_{T_{xj}}\right) \tag{4-55}$$

$$R_{xj} = a_e\left(\pi/2 - \gamma_{xj} - \psi_{R_{xj}}\right) \tag{4-56}$$

where

$$\psi_{xj} = \sin^{-1}\left(\frac{a_e}{a_e + h_{xj}}\right)\cos \gamma_{xj} \tag{4-57}$$

$$\psi_{T_{xj}} = \sin^{-1}\left(\frac{a_e}{a_e + h_{tr}}\right)\cos \gamma_{xj} \tag{4-58}$$

$$\psi_{R_{xj}} = \sin^{-1}\left(\frac{a_e}{a_e + h_{rc}}\right)\cos \gamma_{xj} \tag{4-59}$$

and a_e is the equivalent earth's radius.

Ionospheric Reflection Coefficient. The above search procedure results in the definition of the ionospheric incident angle ϕ_i and the distance from the reflection point to the transmitter, d_i. Linear interpolation is used to define electron and ion density

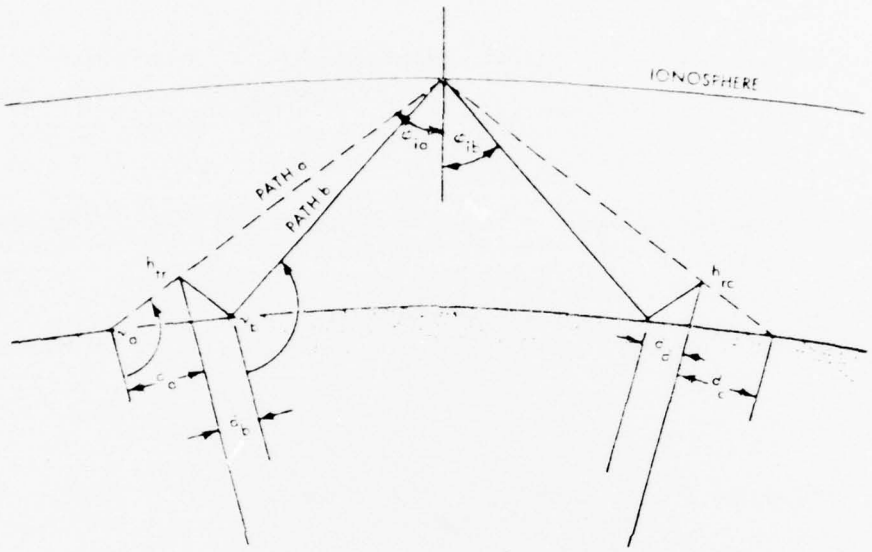

Figure 4-4. Path length geometry for elevated antennas.

profiles, magnetic propagation azimuth, dip angle, and the magnetic field strength at the reflection point. With these quantities determined, the ionospheric reflection coefficients are obtained using procedures described in Section 2.

For elevated antennas, reflection coefficients are computed for only two incident angles, ϕ_{a1} and ϕ_{b1} (see Figure 4-4). Reflection coefficients for path a_1 are used for path a_2, and reflection coefficients for path b_1 are used for path b_2.

Convergence Factors. When the distance between transmitter and receiver is less than the distance to the caustic and a uniform, concentric ionosphere is assumed, the convergence factor for an m-hop ray is (Reference 4-5)

$$\alpha_m = \left(\frac{a_e + h_a}{a_e}\right)\left[\frac{2m \sin(\psi/2m)}{\sin\psi}\right]^{1/2}\left[\frac{h_a + a_e - a_e\cos(\psi/2m)}{(h_a + a_e)\cos(\psi/2m) - a_e}\right]^{1/2} \tag{4-60}$$

where

h_a = ionospheric height (km)

m = number of hops

$\psi = d/a_e$ (radians)

d = ground range between receiver and transmitter (km).

For a nonuniform ionosphere but neglecting any tilt of the ionosphere (ie, the height varies but the ionosphere is locally concentric), it can be shown (see Reference 46) that

$$\alpha_m = \frac{R}{a_e}\left\{\frac{\tan\phi_g}{\sin(d/a_e)}\,\frac{1}{\sum_{I=1}^{m}\frac{1}{2\left[\frac{a_e + h_a(I)}{R(I)}\right]^2\left[1 - \cos\left(\frac{\psi(I)}{2}\right)\left(\frac{a_e}{a_e + h_a(I)}\right)\right]}}\right\}^{1/2} \tag{4-61}$$

where

$h_a(I)$ = the reflection altitude at the Ith reflection point (km)

$R(I)$ = the total ray length for the Ith hop (km)

$\psi(I) = d(I)/a_e$ (radians)

$d(I)$ = the distance along the earth traversed by the Ith hop (km)

$$R = \sum_{I=1}^{m} R(I)$$

ϕ_g = angle of incidence with the earth (radians).

Equations 4-60 and 4-61 indicate an infinite value for the convergence factor when ϕ = 90 degrees. Wait has shown (Reference 4-5) that a correction factor is required as ϕ_g approaches 90 degrees. At a distance near but short of the caustic, the correction factor is

$$C_\alpha \approx 1.34\rho^{1/6} \exp(j\pi/12) , \tag{4-62}$$

where

$$\rho = \frac{ka_e \cos^3 \phi_g}{3 \sin^2 \phi_g} \tag{4-63}$$

The corrected convergence factor is determined from

$$\alpha'_m = C_\alpha \alpha_m \tag{4-64}$$

when

$$0.5 > \rho^{1/3} > 0.05 . \tag{4-65}$$

When $\rho^{1/3} \geq 0.5$, the correction factor is equated to unity. When $\rho^{1/3} \leq 0.05$, the limiting forms given below are used.

For distances beyond the caustic, Wait (Reference 4-5) has shown that

$$\alpha_m = \left(\frac{2m}{\sin\theta}\right)^{1/2} \left\{\left[\left(\frac{a_e + h_a}{a_e}\right)^2 - 1\right]^{1/2} + \frac{d - d_{cm}}{2a_e}\right\}$$

$$\times 1.3466\left(\frac{ka_e}{3}\right)^{1/6} \exp(j\pi/12) , \tag{4-66}$$

where d_{cm} is the distance to the caustic for m hops.

Equation 4-63 is applicable for a uniform ionosphere. For a nonuniform ionosphere, Equation 4-63 is used with the approximation that

$$h_a = \frac{1}{m} \sum_{i=1}^{m} h_a(I) \quad , \tag{4-67}$$

where $h_a(I)$ is the reflection altitude for the Ith hop.

The convergence factors for path a_1 are used for path a_2, and coefficients for path b_1 are used for path b_2.

Ground Reflection Coefficient, Foreground Factors, and Diffraction Loss Terms. The influence of the ground on the propagated signal depends on ray path geometry. The geometric idealizations that are used in computing the influence of the ground at the transmitter location are defined in Figure 4-5.

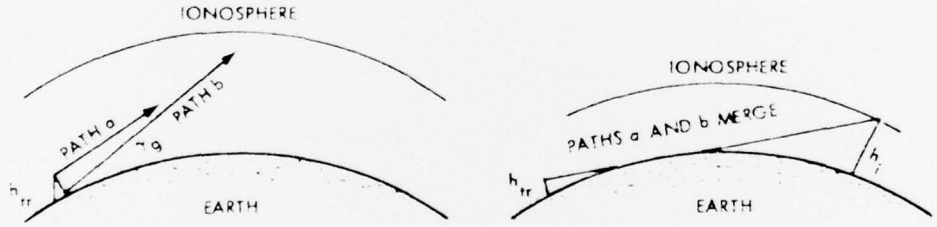

(a) GEOMETRIC OPTICS REGION (b) BEYOND GEOMETRIC OPTICS REGION

Figure 4-5. Geometry to compute the influence of the ground at the transmitter.

When the geometric optics limit applies, the foreground factors for paths a_1 and a_2 are

$$F_{Tj}^{VV} = 1 + R_{gv}\, e^{-jkS_1} \qquad \text{(vertical dipole)} \tag{4-68}$$

$$F_{Tj}^{HB} = 1 + R_{gh}\, e^{-jkS_1} \qquad \text{(horizontal dipole-broadside)} \qquad (4\text{-}69)$$

$$F_{Tj}^{VE} = C\left(1 - R_{gv}\, e^{-jkS_1}\right) \qquad \text{(horizontal dipole-endfire)} \qquad (4\text{-}70)$$

$$S_1 = Sa_2 - Sa_1 \ , \qquad (4\text{-}71)$$

where

Sa_1 = total ray path length (path a_1)

Sa_2 = total ray path length (path a_2) .

In the above equations, the reflection coefficient terms are defined by:

$$R_{gv} = \frac{T_1 - T_2}{T_1 + T_2} \qquad \text{for vertical polarization} \qquad (4\text{-}72)$$

$$R_{gh} = \frac{C - T_2}{C + T_2} \qquad \text{for horizontal polarization} \qquad (4\text{-}73)$$

where

$$T_1 = C\left(\varepsilon_g - \frac{j\sigma_g}{\omega\varepsilon_o}\right)^{1/2} \qquad (4\text{-}74)$$

$$T_2 = \left(\varepsilon_g - \frac{j\sigma_g}{\omega\varepsilon_o} - S^2\right)^{1/2} \qquad (4\text{-}75)$$

ε_o = permittivity of free space (farads/m) (4-76)

ε_g = relative dielectric constant of ground (4-77)

$C = \cos \gamma_g$ (4-78)

$S = \sin \gamma_g$. (4-79)

For paths b_1 and b_2, the foreground factors are

$$F_{Tj}^{VV} = e^{-jkS_2} + R_{gv} \qquad \text{(vertical dipole)} \qquad (4\text{-}80)$$

$$F_{Tj}^{HB} = e^{-jkS_2} + R_{gh} \qquad \text{(horizontal dipole-broadside)} \qquad (4\text{-}81)$$

$$F_{Tj}^{VE} = C\left(e^{-jkS_2} - R_{gv}\right) \qquad (4\text{-}82)$$

$$S_2 = Sb_2 - S_b1 \tag{4-83}$$

where

Sb_1 = total ray path length for path b_1

Sb_2 = total ray path length for path b_2 .

Similar definitions are used for the receiver foreground factors, except that the phase correction terms e^{-jkS_1} and e^{-jkS_2} are not used since the total phase correction is included in the transmitter term.

When the antenna altitude is very small or when the elevation angle at the ground is near zero, paths a_1, a_2, b_1, and b_2 merge and the foreground factors for the composite path are computed from

$$F_{Tj}^{VV} = W_z(y_T, y_i) \qquad \text{(vertical dipole)} \tag{4-84}$$

$$F_{Tj}^{HB} = W_y(y_T, y_i) \qquad \text{(horizontal dipole-broadside)} \tag{4-85}$$

$$F_{Tj}^{VE} = W_z(y_T, y_i) \Big/ \left(\varepsilon_g - \frac{j\sigma_g}{\omega\varepsilon_o}\right)^{1/2} \qquad \text{(horizontal dipole-endfire)} \tag{4-86}$$

The loss functions W_z and W_y are evaluated using Equation 4-10 with

$$y_T = \left(\frac{2}{ka_e}\right)^{1/3} kh_{tr} \tag{4-87}$$

$$y_i = \left(\frac{2}{ka_e}\right)^{1/3} kh_i \ , \tag{4-88}$$

where

h_{tr} = transmitter altitude

h_i = ionosphere reflection altitude for the reflection point nearest the transmitter.

The switch from using Equations 4-68 through 4-83 to using Equations 4-84 through 4-88 is made when $\gamma_g < 0.03$ radians.

Figure 4-6 shows the geometry used for calculating reflection losses or diffraction losses at intermediate ground reflection points.

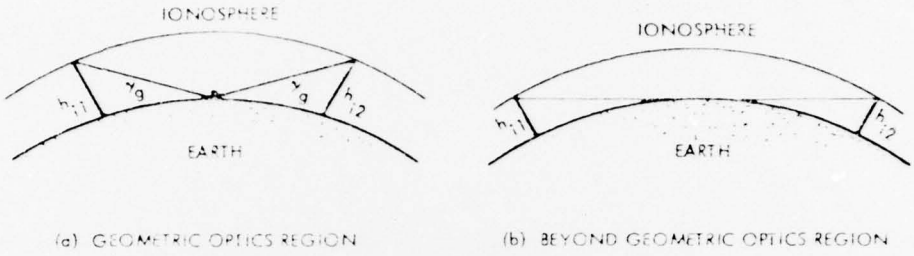

(a) GEOMETRIC OPTICS REGION (b) BEYOND GEOMETRIC OPTICS REGION

Figure 4-6. Geometry to compute the influence of the ground at an intermediate ground reflection point.

Figure 4-6(a) illustrates the case where the receiver is well inside the geometric limit. Here the losses are defined by the Fresnel reflection coefficients given in Equations 4-72 and 4-73. For the situation depicted in Figure 4-6(b), the loss is computed by evaluating Equation 4-8, with y_1 and y_2 defined using h_{i1} and h_{i2}, and X defined using Equation 4-11 and by the distance between adjacent ionospheric reflection points.

REFERENCES

4-1. Wait, J.R., "On the Calculation of the Ground Wave Attenuation Factor at Low Frequencies," *IEEE Transactions on Antennas and Propagation*, pp 515-517, July 1966.

4-2. Bremmer, H., *Terrestrial Radio Waves*, Elsvir Publishing Company, 1949.

4-3. Spies, K.P., and J.R. Wait, *Mode Calculations for VLF Propagation in the Earth-Ionosphere Waveguide*, NBS Technical Note No. 114, U.S. Department of Commerce, Boulder, Colorado, July 1961.

4-4. *Handbook of Mathematical Functions*, Edited by M. Abramowitz and I.A. Stegen, p 446, U.S. Department of Commerce, 1964.

4-5. Wait, J.R., "Diffractive Corrections to the Geometrical Optics of Low-Frequency Propagation," *Electromagnetic Wave Propagation*, pp 87-101, Academic Press, New York, 1960.

4-6. Knapp, W.S., et al, *Eighth Annual Report on Development of Aids for the Study of High-Altitude Nuclear Explosions*, 69TMP-18 (DASA 2285), General Electric-TEMPO, April 1969.

APPENDIX A
DEFINITION OF THE S MATRIX

The elements of the partitioned S matrix (Equations 2-3a through 2-3d) are defined in terms of an intermediate T matrix. The defining equations are (Reference 2-5)

$$S_{11a} = T_{11} + T_{44}$$

$$S_{11b} = T_{14}/C + CT_{41}$$

$$d_{11a} = T_{11} - T_{44}$$

$$d_{11b} = T_{14}/C - CT_{41}$$

$$S_{12} = T_{12}/C + T_{42}$$

$$d_{12} = T_{12}/C - T_{42}$$

$$S_{21} = T_{31} + T_{34}/C$$

$$d_{21} = T_{34}/C - T_{31}$$

$$S_{22} = C + T_{32}/C$$

$$d_{22} = C - T_{32}/C \ ,$$

where

$C = \cos\theta$

$S = \sin\theta$

θ = complex angle of incidence (deg)

and the intermediate matrix T relates the electromagnetic field components to their derivatives. In turn, T is defined in terms of the susceptibility matrix M:

$$\underline{T} = \begin{bmatrix} \left(-\frac{SM_{31}}{1+M_{33}}\right) & \left(\frac{SM_{32}}{1+M_{33}}\right) & (0) & \left(\frac{C^2+M_{33}}{1+M_{33}}\right) \\ (0) & (0) & (1) & (0) \\ \left(\frac{M_{23}M_{31}}{1+M_{33}}-M_{21}\right) & \left(C^2+M_{22}-\frac{M_{23}M_{32}}{1+M_{33}}\right) & (0) & \frac{SM_{23}}{1+M_{33}} \\ \left(1+M_{11}-\frac{M_{13}M_{31}}{1+M_{33}}\right) & \left(\frac{M_{32}M_{13}}{1+M_{33}}-M_{12}\right) & (0) & -\frac{SM_{13}}{1+M_{33}} \end{bmatrix}$$

Finally, the susceptibility $\underline{M}$ matrix is defined as

$$\underline{M} = \frac{-X}{U(U^2-Y^2)} \begin{bmatrix} (U^2-\ell^2Y^2) & (-jUnY-\ell mY^2) & (jUmY-\ell nY^2) \\ (jUnY-\ell mY^2) & (U^2-m^2Y^2) & (-jU\ell Y-mnY^2) \\ (-jUmY-\ell nY^2) & (jU\ell Y-mnY^2) & (U^2-n^2Y^2) \end{bmatrix}$$

$$- \begin{bmatrix} (-2[D-z]/a) & 0 & 0 \\ 0 & (-2[D-z]/a) & 0 \\ 0 & 0 & (-2[D-z]/a) \end{bmatrix}$$

where

$j = \sqrt{-1}$

$X = (\omega_p/\omega)^2$

$U = 1 - j(\nu/\omega)$

$Y = \mu_o \omega_m/\omega$ ((henrys)

ω_m = magnetic gyrofrequency (s^{-1})

ω_p = plasma frequency (s^{-1})

$\ell = \cos\theta_D \cos\phi_a$

$m = \cos\theta_D \sin\phi_a$

$n = -\sin \theta_D$

ν = collision frequency (s^{-1})

ω = wave frequency (s^{-1})

μ_o = free space permeability (henrys/m)

θ_D = magnetic dip angle (deg)

a = earth's radius (km)

D = altitude where index of refraction is unity (km)

ϕ_a = direction of propagation east of magnetic north (deg)

z = altitude (km) .

The matrix $\underline{M}$ described above is general in that it represents a single ionospheric constituent. Three species are considered by this model: electrons and positive and negative ions. Thus for each species there will be a matrix $\underline{M}_i$, and the matrix elements needed for computing the $\underline{T}$ matrix elements are found from

$$\underline{M} = \sum_{i=1}^{3} \underline{M}_i \ .$$

APPENDIX B

STARTING SOLUTION FOR THE ANISOTROPIC INTEGRATION TECHNIQUE

Closed-form expressions* for starting values for the reflection coefficient integration are obtained by first finding the two upgoing wave solutions, q_1 and q_2, of the Booker quartic

$$q^4 + 4b_3q^3 + 6b_2q^2 + 4b_1q + b_0 = 0 \ . \qquad \text{(B-1)}$$

The parameter q is equal to the product of the index of refraction and the cosine of the angle of refraction in the ionosphere, and the coefficients are functions of the susceptibility matrix $\underline{M}$:

$$b_3 = B_3/(4B_4)$$

$$b_2 = B_2/(6B_4)$$

$$b_1 = B_1/(4B_4)$$

$$b_0 = B_0/B_4$$

$$B_4 = (1 + M_{33})$$

$$B_3 = S(M_{13} + M_{31})$$

$$B_2 = -(C^2 + M_{33})(1 + M_{11}) + M_{13}M_{31} - (1 + M_{33})(C^2 + M_{22}) + M_{23}M_{32}$$

$$B_1 = S[M_{12}M_{23} + M_{21}M_{32} - (C^2 + M_{22})(M_{13} + M_{31})]$$

$$B_0 = (1 + M_{11})(C^2 + M_{22})(C^2 + M_{33}) + M_{12}M_{23}M_{31} + M_{13}M_{21}M_{32} - M_{13}(C^2 + M_{22})M_{31} - (1 + M_{11})M_{23}M_{32} - M_{12}M_{21}(C^2 + M_{33}) \ .$$

*From Reference 2-3.

Preceding page blank

The $\underline{R}$ matrix elements are then determined from

$$
\begin{aligned}
{}_{u}R_{u} &= [(T_1C - P_1)(C + q_q) - T_2C - P_2)(C + q_1)]/\Delta \\
{}_{1}R_{1} &= [T_1C + P_1)(C - q_2) - (T_2C + P_2)(C - q_1)]/\Delta \\
{}_{1}R_{u} &= -2C(T_1P_2 - T_2P_1)/\Delta \\
{}_{u}R_{1} &= -2C(q_1 - q_2)/\Delta
\end{aligned}
$$

where for i = 1.2

$$
\begin{aligned}
\Delta &= (T_1C + P_1)(C + q_2) - (T_2C + P_2)(C + q_1) \\
T_i &= q_iP_i - S(-D_{11,i}D_{32} + D_{12}D_{31,i})/\Delta_i \\
P_i &= (-D_{12}D_{33} + D_{13,i}D_{32})/\Delta_i \\
\Delta_i &= D_{11,i}D_{33} - D_{13,i}D_{31,i} \\
D_{11,i} &= 1 + M_{11} - q_i^2 \\
D_{12} &= M_{12} \\
D_{13,i} &= M_{13} + q_iS \\
D_{13,i} &= M_{31} + q_iS \\
D_{32} &= M_{32} \\
D_{33} &= C^2 + M_{33} .
\end{aligned}
$$

APPENDIX C
GROUND REFLECTION COEFFICIENTS

The symbols $\bar{R}$ represent the ground reflection coefficients referenced to the altitude where the ionospheric reflection coefficient computations are terminated. They are defined as follows:

$$ {}_{\perp}\bar{R}_{\perp} = \frac{A_1 - A_2}{A_1 + A_2} \qquad \text{(C-1)} $$

$$ {}_{\parallel}\bar{R}_{\parallel} = \frac{A_3 + A_4}{A_3 - A_4} , \qquad \text{(C-2)} $$

where

$$ A_1 = Cn_H^2(A_{11} + A_{12}) \qquad \text{(C-3)} $$

$$ A_2 = A_{21} + A_{22} \qquad \text{(C-4)} $$

$$ A_3 = A_{31} + A_{32} \qquad \text{(C-5)} $$

$$ A_4 = C(A_{41} + A_{42}) . \qquad \text{(C-6)} $$

In Equations C-3 through C-6,

C = cosine of the eigenangle

$$ n_H^2 = 1 - 2(D - z_{bot})/a , $$

where

D = reference altitude where the index of refraction is unity

z_{bot} = altitude where ionospheric reflection coefficient calculations are terminated.

The double subscripted A's are defined in terms of Airy functions, W_1 and W_2, of the first and second kind as defined by Wait

in Reference 3-2. In Equations C-7 through C-14, primes indicate derivatives with respect to the argument.

$$A_{11} = W_2(t_H)[W_1'(t_o) - QW_1(t_o)] \quad \text{(C-7)}$$

$$A_{12} = W_1(t_H)[W_2'(t_o) - QW_2(t_o)] \quad \text{(C-8)}$$

$$A_{21} = \frac{j}{k_a}[W_2'(t_H) - 1/(2k_a^2)W_2(t_H)][W_1'(t_o) - QW_1(t_o)] \quad \text{(C-9)}$$

$$A_{22} = \frac{j}{k_a}[W_1'(t_H) - 1/(2k_a^2)W_1(t_H)][W_2'(t_o) - QW_2(t_o)] \quad \text{(C-10)}$$

$$A_{31} = S_2(t_H)[-jW_1'(t_o)/k_a + (n_g^2 - S^2)^{1/2}W_1(t_o)] \quad \text{(C-11)}$$

$$A_{32} = W_1'(t_H)[-jW_2'(t_o)/k_a + (n_g^2 - S^2)^{1/2} W_2(t_o)] \quad \text{(C-12)}$$

$$A_{41} = W_2(t_H)[W_1'(t_o) + jk_a(n_g^2 - S^2)^{1/2} W_1(t_o)] \quad \text{(C-13)}$$

$$A_{42} = -W_1(t_H)[W_2'(t_o) + jk_a(n_g^2 - S^2)^{1/2} W_2(t_o)] , \quad \text{(C-14)}$$

where

$$k_a = \left(\frac{ka}{2}\right)^{1/3} \quad \text{(C-15)}$$

$$t = t(z) = - k_a^2(C^2 - 2(D - z)/a) \quad \text{(C-16)}$$

$t_o = t(o)$

$t_H = t(z_{bot})$

$n_g^2 = (\varepsilon - j\frac{\sigma}{\omega\varepsilon_o})$

$Q = n_o^2 Q_H/n_g^2 + 1/(2k_a^2)$

$n_o^2 = 1 - 2D/a$

$Q_H = -jk_a(n_g^2 - S^2)^{1/2}$

z = altitude (km)

a = earth's radius (km) .

END

DATE
FILMED

8 — 81

DTIC